การศึกษาเชิงทฤษฎีของไฮโดรฟอสโฟนิเลชันของแอลดีไฮด์เร่งปฏิกิริยาด้วยกรดในน้ำ

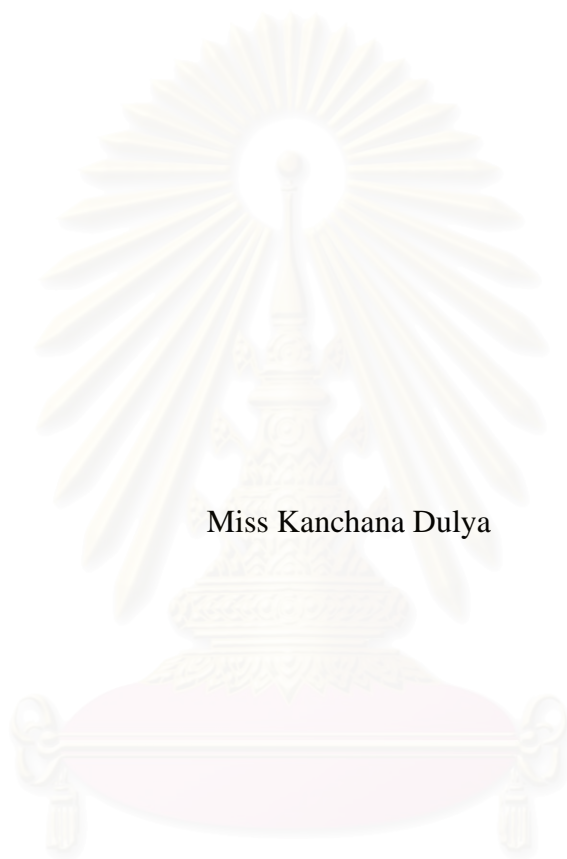นางสาว กาญจนา ดุลยา

วิทยานิพนธ์นี้เป็นส่วนหนึ่งของการศึกษาตามหลักสูตรปริญญาวิทยาศาสตรมหาบัณฑิต
สาขาวิชาปิโตรเคมีและวิทยาศาสตร์พอลิเมอร์
คณะวิทยาศาสตร์   จุฬาลงกรณ์มหาวิทยาลัย
ปีการศึกษา 2549

THEORETICAL STUDY OF HYDROPHOSPHONYLATION OF ALDEHYDES

CATALYZED BY ACID IN WATER

Miss Kanchana Dulya

A Thesis Submitted in Partial Fulfillment of the Requirements

for the Degree of Master of Science Program in Petrochemistry and Polymer Science

Faculty of Science

Chulalongkorn University

Academic Year 2006
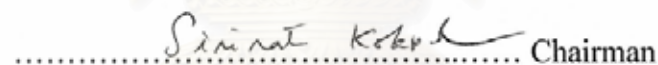
**Thesis Title**        THEORETICAL STUDY OF HYDROPHOSPHONYLATION OF ALDEHYDES CATALYZED BY ACID IN WATER

**By**        Miss Kanchana Dulya

**Field of study**        Petrochemistry and Polymer Science

**Thesis Advisor**        Associate Professor Vithaya Ruangpornvisuti, Dr.rer.nat.

---

Accepted by the Faculty of Science, Chulalongkorn University in Partial Fulfillment of the Requirements for the Master's Degree

……………………………………… Dean of the Faculty of Science

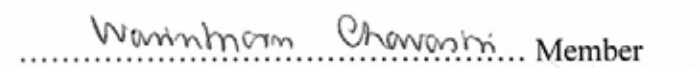(Professor Piamsak Menasveta, Ph.D.)

THESIS COMMITTEE

……………………………………… Chairman

(Associate Professor Sirirat Kokpol, Ph.D.)

……………………………………… Thesis Advisor

(Associate Professor Vithaya Ruangpornvisuti, Dr.rer.nat.)

……………………………………… Member

(Associate Professor Nuanphun Chantarasiri, Ph.D.)

……………………………………… Member

(Assistant Professor Dr. Warinthon Chavasiri, Ph.D.)

กาญจนา  ดุลยา:  การศึกษาเชิงทฤษฎีของไฮโดรฟอสโฟนิเลชันของแอลดีไฮด์เร่งปฏิกิริยา
ด้วยกรดในน้ำ (THEORETICAL STUDY OF HYDROPHOSPHONYLATION
OF ALDEHYDES CATALYZED BY ACID IN WATER)
อ. ที่ปรึกษา : รศ. ดร. วิทยา เรืองพรวิสุทธิ์, 81 หน้า.

การคำนวณโครงสร้างที่เหมาะสมของสปีชีส์ต่างๆที่เกี่ยวข้องในปฏิกิริยาการเปลี่ยนแอลดี
ไฮด์เป็นแอลฟาไฮดรอกซีฟอสโฟเนตโดยวิธี B3LYP/6-31G(d)  และ  B3LYP/6-311+G(d,p)
โดยได้แสดงพลังงานและสมบัติทางเทอร์โมไดนามิกส์ของกลไกการเกิดปฏิกิริยาโดยใช้กรดเป็น
ตัวเร่งปฏิกิริยา การคำนวณหาค่าคงที่ ณ อุณหภูมิ 298.15   เคลวิน ซึ่งเป็นขั้นตอนการกำหนด
อัตราเร่งในระบบที่เป็นก๊าซและสารละลายน้ำของสารตั้งต้นทั้งสองชนิด อันได้แก่ อะซีทัลดีไฮด์
และไอโซโพรพิลแอลดีไฮด์

| สาขาวิชา | ปิโตรเคมีและวิทยาศาสตร์พอลิเมอร์ | ลายมือชื่อนิสิต | |
| ปีการศึกษา | 2549 | ลายมือชื่ออาจารย์ที่ปรึกษา | |

# 4873401923: PETROCHEMISTRY AND POLYMER SCIENCE PROGRAM

KEY WORD: ALDEHYDES/ α-HYDROXY PHOSPHONATE/ DFT

KANCHANA DULYA: THEORETICAL STUDY OF HYDROPHOSPHO-NYLATION OF ALDEHYDES CATALYZED BY ACID IN WATER. THESIS ADVISOR: ASSOC. PROF. VITHAYA RUANGPORNVISUTI, Dr.rer.nat., 81 pp.


The geometrical optimizations of all involved species in conversions of aldehydes to α-hydroxy phosphonate derivatives were carried out using the B3LYP/6-31G(d) and B3LYP/6-311+G(d,p) methods. Mechanisms of these conversion reactions in acid-catalyzed solutions in terms of energetic and thermodynamic properties are reported. Rate constants at 298.15 K, determining-steps, in gaseous and aqueous phases for both acetaldehyde and $i$-propyl aldehyde conversions were obtained.

Field of study  Petrochemistry and Polymer Science  Student's signature  K. Dulya

Academic year  2006  Advisor's signature

# ACKNOWLEDGEMENTS

I would like to express my sincere gratitude to my advisor Associate Professor Dr.Vithaya Ruangpornvisuti for his continuous attention and guidance thought the years of my study. I deeply appreciate suggestion and comments of my committee members, Associate Professor Dr. Sirirat Kokpol, Associate Professor Dr. Nuanphun Chantarasiri and Assistant Professor Dr. Warinthon Chavasiri.

The greatest thanks are extended to Mr. Banchob Wano who always assists intensive quantum and computational chemistry details. Moreover, I greatly appreciated the Petrochemistry and Polymer Science Program and Graduate School Chulalongkorn University for research grant.

Special thanks to all members in Associate Professor Dr. Vithaya Ruangpornvisuti's group for their worthy comments, valuable suggestions and encouragement I also would like to thanks all my friends at Chulalongkorn University for their friendship throughout my study.

Finally, I would like to dedicate this to my parents, Promma and Vithoon Dulya for their love, understanding and support for me is priceless. Without them, I would never be able to achieve this goal.

# CONTENTS

# LIST OF FIGURES

**Figure**                                                                      **Page**

# LIST OF TABLES

# CHAPTER I

# INTRODUCTION

## 1.1 Background

The phosphoryl group is a fundamental significance in many of the most important molecules that controls molecular replication, cell biochemistry and metabolic process in all living species *[1]*. Succeeding the more extensively studied α-amino phosphoryl compounds, α-hydroxy phosphonates compounds have recently been proved to be biologically active and have been shown to inhibit the enzymes rennin and HIV protease. *[2-3]* Therefore, a large number of thio (seleno) phosphase-phosphonate derivatives, bearing a P-O-C-P bone structure, were synthesized and their significant herbicidal, antiviral and fungicidal activities were reported for the first time.

In addition, α-hydroxy phosphonates are useful intermediates in the synthesis of other substituted phosphonates and represent an interesting chiron for the preparation of the parent α-amino phosphonic acids *[4]*, which are compounds attracting increased interested in medicinal chemistry. Moreover, α-hydroxy phosphonic acid derivatives have been proved to act as a hydrolytically stable mimic of phosphoric acid esters; some benzylic α-hydroxy phosphonic acid derivatives have been shown to possess potential inhibitory activity towards EPSP synthase *[5]* and tyrosine-specific protein kinase. All of this advancetages make this synthesis reaction practical for large-scale α-hydroxy phosphonates production.

In the past, the α-hydroxy phosphonates were synthesized and determined by NMR spectroscopy of the O-methyl mandelate ester derivatives *[6]* and a solid phase method *[7]*. Enantioselective α-hydroxy phosphonates were synthesized using the LaLi$_3$tris (binaphthoxide) catalyst *[8]*, via oxidation with (camphorsulfonyl)oxairidines *[9]*. Resin-bound *N*-acylate amino acid aldehydes converted in a single step to α-hydroxy phosphonates were reported *[10]*. Titanium alkoxide-catalyzed asymmetric

phosphonylation of aldehyde convered to hydroxy phosphonate were carried out and reported *[11]*.

Traditional solution phase synthesis of α-hydroxy phosphonates include, thermal non-catalyzed addition, the reaction of a trialkylphosphite with an aldehyde in the presence of a Lewis acid or alumina *[12]*, and the nucleophilic addition of dialkyl H-phosphonate with carbonyls (Pudovik reaction), which is promoted by strong bases (NaH,LDA,n-BuLi,etc.,).An alternative method is the reaction of a tris (trimethylsilyl) phosphate with a carbonyl in the presence of a Lewis acid. Cesium-uoride is also a feasible catalyst.

However, these methods have some disadvantages. For example, in the strongly alkaline medium used, α-hydroxy-alkanephosphonic esters are cleaved to regenerate the starting carbonyl compounds. In addition, the yields are not always good and mixtures of products are sometimes obtained. Hence, there is a need to develop a convenient, environmentally benign and feasible method for the synthesis of α-hydroxy phosphonates.

Recently, hydrophosphonylation of aldehydes catalyzed guanidine hydrochloride in water *[13]* were studied that the reaction of aliphatic and aromatic aldehydes with trimethylphosphite gave higher yields in shorter time with no harmful effect to the environment. Its mechanism and a quantum model of this reaction's transfer is interesting and is proposed in this study.

In 1999 Jursic *[14]* studied about hydronium ion addition to ethylene by ab initio computational method. Their stabilization energies, enthalpies of the reaction and activation energies are evaluated and found that the formation of the ethylene–hydronium ion associate is a minimum on the potential energy surface for the ethylene1hydronium ion-protonated ethanol potential. In addition, the DFT method can estimated values of proton affinity for ethylene and ethanol closest to the experimental values.

## 1.2 Hydrophosphonylation reaction

The reaction of aldehyde and trimethylphosphite were examined as follow
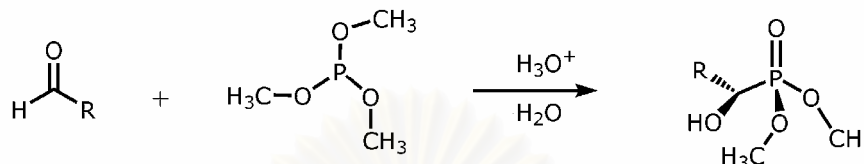


**Figure 1.1** A representative scheme of aldehyde hydrophosphonylation *[13].*

The mechanism of this reaction is tentatively postulated in Figure 1.2. It seems that guanidine hydrochloride in the water generates a hydronium ion, which accelerates the reaction. The reaction may thus proceed *via* an active cationic species [C=OH]$^+$ This indicates that the carbonyl oxygen is protonated, generating a [C=OH]$^+$ species and thereby slightly reducing the electron density at carbonyl carbon. The electron densities at the other carbon atoms are affected to a smaller extent. The results suggest that the reaction further proceeds by the addition of trimethyl phosphate that would generate to form intermediate, which was then treated with water to afford the desired compounds of α-hydroxy phosphonates
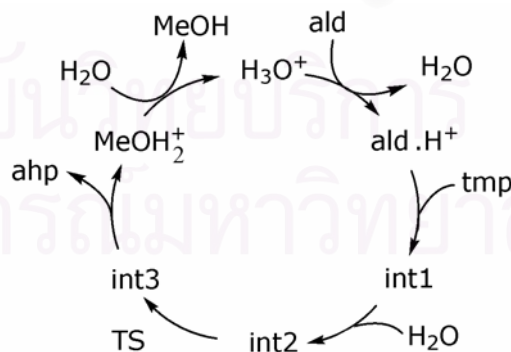


**Figure 1.2** The mechanism of aldehyde conversions to α-hydroxy phosphonates (ahp) in acid-catalyzed system

**1.3 Objective**

In this work, we have investigated molecular structures of all species involved in conversions of aldehydes to α-hydroxyl phosphates in acid-catalyzed system and their mechanisms in gaseous and aqueous phases by quantum calculated. Aldehyde reactants studied in this work are acetaldehyde and *i*-propyl aldehyde. Energetics and thermodynamic properties of their mechanistic reactions have been determined by density functional theory at B3LYP/6-31G(d) and B3LYP/6-311+G(d,p) levels of theory.

# CHAPTER II

# THEORETICAL BACKGROUND

## 2.1 Introduction to Quantum Mechanics

The word quantum comes from Latin (quantum, "how much?") and is first used by Max Plank in 1900 to donate the constrained quantities or amounts in which energy can be emitted or absorbed. "Mechanics" as used in physics is traditionally the study of the behavior of bodies under the action of forces. The term "quantum mechanics" is apparently first used by Born (of the Born-Oppenheimer approximation) in 1924. Because of molecules are consisted of nuclei and electrons, quantum chemistry deals with the motion of electrons under the influence of the electromagnetic force exerted by nuclear charges. An understanding of the behavior of electrons in molecules, structures and reactions of molecules, reset on quantum mechanics and in particular on the adornment of quantum chemistry, the Schrödinger equation *[15]*.

## 2.2 Solution of the Schrödinger Equation of Molecular Systems

### 2.2.1 The Schrödinger Equation

The ultimate goal of most quantum chemical approaches is the approximate solution of the time-independent, non-relativistic Schrödinger equation:

$$\hat{H}\psi_i(\vec{x}_1,\vec{x}_2,...,\vec{x}_N,\vec{R}_1,\vec{R}_2,...,\vec{R}_M) = _i\psi_i(\vec{x}_1,\vec{x}_2,...,\vec{x}_N,\vec{R}_1,\vec{R}_2,...,\vec{R}_M) \qquad (2.1)$$

where $\hat{H}$ is the Hamilton operator for a molecular system consisting of M nuclei and N electrons in the absence of magnetic or electric fields. $\hat{H}$ is a differential operator representing the total energy:

$$\widehat{H} = -\frac{1}{2}\sum_{i=1}^{N}\nabla_i^2 - \frac{1}{2}\sum_{A=1}^{M}\frac{1}{M_A}\nabla_A^2 - \sum_{i=1}^{N}\sum_{A=1}^{M}\frac{Z_A}{r_{iA}} + \sum_{i=1}^{N}\sum_{j>i}^{N}\frac{1}{r_{ij}} + \sum_{A=1}^{M}\sum_{B>A}^{M}\frac{Z_A Z_B}{R_{AB}} \qquad (2.2)$$

Here, A and B run over the M nuclei while i and j denote the N electrons in the system. The first two terms describe the kinetic energy of the electrons and nuclei respectively, where the Laplacian operator $\nabla_q^2$ is difinied as a sum of differential operators (in cartesian coordinates):

$$\nabla_q^2 = \frac{\partial^2}{\partial x_q^2} + \frac{\partial^2}{\partial y_q^2} + \frac{\partial^2}{\partial z_q^2} \qquad (2.3)$$

$M_A$ is the mass of nucleus A in multiples of the mass of an electron. The remaining three terms define the potential parts of the Hamiltonian and represent the attractive electrostatic interaction between the nuclei and the electrons and the repulsive potential due to electron-electron and nucleus-nucleus interactions, respectively. $R_{pq}$ (and similarly $R_{qp}$) is the distance between the particles p and q, i.e., $r_{pq} = \left|\vec{r}_p - \vec{r}_q\right|$. $\psi_i(\vec{x}_1, \vec{x}_2, ..., \vec{x}_N, \vec{R}_1, \vec{R}_2, ..., \vec{R}_M)$ stands for the wave function of the i'th state of the system, which depends on the 3N spatial coordinates $\{\vec{r}_i\}$, and the N spin coordinates $\{S_I\}$ of the electrons, which are collectively termed $\{\vec{x}_i\}$, and the 3M spatial coordinates of the nuclei, $\{\vec{R}_I\}$. The wave function $\psi_i$ contains all information that can possibly be known about the quantum system at hand. Finally, $E_I$ is the numerical value of the energy of the state described by $\psi_i$.

All equations given in this text appear in a very compact form, without any fundamental physical constants. We achieve this by employing the so-called system of atomic units, which is particularly adapted for working with the atoms and molecules. In this system, physical quantities are expressed as multiples of fundamental constants and, if necessary, as combinations of such constants. The mass of an electron, $m_e$, the modulus of its charge, $|e|$, Planck's constant $h$ divided by $2\pi$, $\hbar$, and $4\pi$, $\varepsilon_0$, the permittivity of the

vacuum, are all set to unity. Mass, charge, action etc. are then expressed as multiples of these constants, which can therefore be dropped from all equations *[15]*.

### 2.2.2 Born-Oppenheimer Approximation

The Schrödinger equation can be further simplified if we take advantage of the significant differences between the masses of nuclei and electrons. Even the lightest of all nuclei, the proton ($^1$H), weighs roughly 1800 times more than an electron. Thus, the nuclei move much slower than the electrons. The practical consequence is that we can at least to a good approximation take the extreme point of view and consider the electrons as moving in the field of fixed nuclei. This is the famous *Born-Oppenheimer* or clamped-nuclei approximation. If the nuclei and fixed in space and do not move, their kinetic energy is zero and the potential energy due to nucleus-nucleus repulsion is merely a constant. Thus, the complete Hamiltonian given in equation (2.4) reduces to the so-called electronic Hamiltonian:

$$\widehat{H}_{elec} = \frac{1}{2}\sum_{i=1}^{n}\nabla_i^2 - \sum_{i=1}^{n}\sum_{A=1}^{K}\frac{Z_A}{r_{iA}} + \sum_{i=1}^{n}\sum_{j>1}^{n}\frac{1}{r_{ij}} \tag{2.4}$$

The solution of the Schrödinger equation with $\widehat{H}_{elec}$ is the electronic wave function $\psi_{elec}$ and the electronic energy $E_{elec}$. $\psi_{elec}$ depends on the electron coordinates, while the nuclear coordinates enter only parametrically and do not explicity appear in $\psi_{elec}$. The total energy $E_{tot}$ is then the sum of $E_{elec}$ and the constant nuclear repulsion term *[16]*:

$$E_{nuc} = \sum_{A=1}^{K}\sum_{B>A}^{M}\frac{Z_A Z_B}{r_{AB}} \tag{2.5}$$

$$\widehat{H}_{elec}\psi_{elec} = E_{elec}\psi_{elec} \tag{2.6}$$

and

$$E_{tot} \quad = \quad E_{elec} + E_{nuc} \tag{2.7}$$

The attractive potential exerted on the electrons due to the nuclei – the expectation value of the second operator $\widehat{V}_{Ne}$ in equation (2.4) is the often termed the external potential, $V_{ext}$ , in density functional theory, even though the external potential is not necessarily limited to the nuclear field but may include external magnetic or electric fields etc. From now on we will only consider the electronic problem of equations (2.4)-(2.6) and the subscript "elec" will be dropped.

## 2.3 The Hartree-Fock Method

The Hartree-Fock method seeks to approximately solve the electronic Schrödinger equation, and it assumes that the wave function can be approximated by a single Slater determinant made up of one spin orbital per electron. Since the energy expression is symmetric, the variation theorem holds, and so we know that the Slater determinant with the lowest energy is as close as we can get to the true wave function for the assumed functional form of a single Slater determinant. The Hartree-Fock method determines the set of spin orbitals which minimize the energy and give us this best single determinant. So, we need to minimize the Hartree-Fock energy expression with respect to changes in the orbitals:

$$\chi_i \rightarrow \chi_i + {}^{\delta}\chi_i \tag{2.8}$$

We have also been assuming that the orbitals are orthonormal, and we want to ensure that our variational procedure leaves them orthonormal. The Hartree-Fock equations can be solved numerically (exact Hartree-Fock), or they can be solved in the space spanned by a set of basis functions (Hartree-Fock-Roothan equations). In either case, note that the solutions depend on the orbitals. Hence, we need to guess some initial

orbitals and then refine our guesses iteratively. For this reason, Hartree-Fock is called a *self-consistent-field* (SCF) approach.

The first term above in square brackets:

$$\sum_{j \neq i} \left[ \int dx_2 \left| \chi_j(x_2) \right|^2 r_{12}^{-1} \right] \chi_i(x_1), \tag{2.9}$$

gives the Coulomb interaction of an electron in spin orbital $\chi_i$ with the average charge distribution of the other electrons. Here we see in what sense Hartree-Fock is a mean field theory. This is called the *Coulomb term*, and it is convenient to define a Coulomb operator as:

$$J_j(x_1) = \int dx_2 \left| \chi_j(x_2) \right|^2 r_{12}^{-1}, \tag{2.10}$$

which gives the average local potential at point $x_1$ due to the charge distribution from the electron in orbital $\chi_j$.

We can define an exchange operator in terms of its action on an arbitrary spin obital $\chi_i$ :

$$K_j(x_1)\chi_i(x_1) = \left[ \int dx_2 \chi_j^*(x_2) r_{12}^{-1} \chi_i(x_2) \right] \chi_j(x_1). \tag{2.11}$$

Introducing a basis set transforms the Hartree-Fock equations into the Roothaan equations. Denoting the atomic orbital basis functions as $\overline{\chi}$ , we have the expansion:

$$\chi_i = \sum_{\mu=1}^{K} C_{\mu i} \overline{\chi}_\mu \tag{2.12}$$

for each spin orbital $i$. This leads to:

$$f(x_1) \sum_v C_{vi} \tilde{\chi}_v(X_1) = \in_i \sum_v C_{vi} \tilde{\chi}_v(X_1). \tag{2.13}$$

This can be simplified by introducing the matrix element notation :

$$S_{\mu\nu} = \int dx_1 \, \overline{\chi}_\mu^*(x_1) \overline{\chi}_\nu(x_1),$$

(2.14)

$$F_{\mu\nu} = \int dx_1 \, \overline{\chi}_\mu^*(x_1) \overline{\chi}_\nu(x_1).$$

(2.15)

Now the Hartree-Fock-Roothaan equations can be written in matrix form as:

$$\sum_\nu F_{\mu\nu} C_{\nu i} = \in_i \sum_\nu S_{\mu\nu} C_{\nu i}$$

(2.16)

or even more simply as matrices:

$$\mathbf{FC} = \mathbf{SC} \in$$

(2.17)

where $\in$ is a diagonal matrix of the orbital energies $\in_i$. This is like an eigenvalue equation except for the overlap matrix S. One performs a transformation of basis to go to an orthogonal basis to make S vanish. Then it's just a matter of solving an eigenvalue equation Well, not quite. Since F depends on it's own solution (through the orbitals), the process must be done iteratively. This is why the solution of the Hartree-Fock-Roothaan equations are often called the self-consistent-field procedure *[16]*.

## 2.4 Basis Sets

The approximate treatment of electron-electron distribution and motion assigns individual electrons to one-electron function, termed *spin orbital*. These consist of a product of spatial functions, termed *molecular orbitals (MO)*, $\psi_1(x, y, z)$, $\psi_2(x, y, z)$, $\psi_3(x, y, z)$, ..., and either $\alpha$ or $\beta$ spin components. The spin orbitals are allowed complete freedom to spread throughout the molecule. Their exact forms are determined to minimize the total energy. In the simplest level of theory, a single assignment of electron to orbital is made by used $\psi$ as atomic orbital wavefunction based on the Schrödinger

equation for the hydrogen atom. This is not a suitable approach for molecular calculation. This problem can be solved by representing MO as linear combination of basis functions.

In practical calculation, the molecular orbitals $\psi 1$, $\psi 2$, ..., are further restricted to be linear combinations of a set of $N$ known one-electron function $\phi_1(x,y,z)$, $\phi_2(x,y,z)$, ..., $\phi_N(x,y,z)$:

$$\psi_i = \sum_{\mu=1}^{N} c_{\mu i} \phi_\mu \qquad (2.18)$$

The functions $\phi_1$, $\phi_2$, ..., $\phi_N$, which are defined in the specification of the model, are known as one-electron basis function called basis function. The set of basis functions is called basis set. If the basis functions are the atomic orbitals for the atoms making up the molecule, function in equation 2.18 is often described as the *linear combination of atomic orbitals* (LCAO). There are two types of basis function which commonly used in the electronic structure calculations, *Slater type orbitals* (STO) and *Gaussian type orbitals* (GTO).

The Slater orbitals are primarily used for atomic and diatomic systems where high accuracy is required and semiempirical calculations where all three- and four-center integrals are neglected. The Slater type orbitals have the function form:

$$b = Ae^{-\varsigma r} r^{n^*-1} Y_{lm}(\theta,\phi) \qquad (2.19)$$

where parameter $n^*$ and $\xi$ are chosen to make the larger part of the orbitals look like atomic Hartree-Fock orbitals. There are a lot like hydrogen orbitals, but without the complicated nodal structure.

The Gaussian type orbitals can be written in terms of polar or cartesian coordinates:

$$g = x^a y^b z^c e^{-\alpha r^2} Y_{lm}(\theta,\phi) \qquad (2.20)$$

in which *a*, *b*, and *c* are integers and $\alpha$ is a parameter that is usually fixed. Primitive Gaussian function is shown in equation 2.20. Normally, several of these Gaussian functions are summed to define more realistic atomic orbitals basis functions, as shown below:

$$b_\mu = \sum_p k_{\mu p}\, g_p.$$ 

(2.21)

The coefficients $k_{\mu p}$ in this expansion are chosen to make the basis functions look as much like Slater orbitals as possible. Slater functions are good approximation to atomic wavefunctions but required excessive computer time more than Gaussian functions, while single-Gaussian functions are a poor approximation to the nearly ideal description of an atomic wavefunction that Slater function provides. The solution to the problem of this poor functional behavior is to use several Gaussians to approximate a Slater function. In the simplest version of this basis, n Gaussian functions are superimposed with fixed coefficients to form one-Slater type orbital. Such a basis is denoted STO-nG, and n = 3, 4.

The limit of quantum mechanics involves an infinite set of basis function. This is clearly impractical since the computational expanse of molecular orbital calculations is proportional to the power of the total number of basis functions.  Therefore, ultimate choice of basis set size demands on a compromise between accuracy and efficiency. The classification of basis sets is given below.

### 2.4.1 Minimal Basis Sets

The minimum basis set is a selected basis function for every atomic orbital that is required to describe the free atom. For hydrogen atom, the minimum basis set is just one *1s* orbital. But for carbon atom, the minimum basis set consisted of a *1s* orbital, a *2s* orbital and the full set of three *2p* orbitals. For example, the minimum basis set for the methane molecule consists of 4 *1s* orbitals, one per hydrogen atom, and the set of *1s*, *2s* and *2p* orbitals described above for carbon. Thus, total basis set comprises of 9 basis functions.

Several minimum basis sets are used as common basis sets especially the STO-nG basis sets because they are available for almost all elements in the periodic table. The most common of minimum basis sets is STO-3G, where a linear combination of three Gaussian type orbitals (GTOs) is fitted to a Slater-type orbital (STO). The individual GTOs are called primitive orbitals, while the combined functions are called contracted functions. For example, the STO-3G basis set for methane consists of a total of 9 contracted functions built from 27 primitive functions. Other commonly uses of STO-nG basis sets are STO-4G and STO-6G where each STO is fitted to 4 and 6 GTOs, respectively.

### 2.4.2 Scaled Orbital by Splitting the Minimum Basis Sets

In the early calculation on the hydrogen molecule, it is discovered that the STO *1s* orbitals do not give the best result in the molecular environment when the Schrödinger equation is solved, because electron is attracted to both nuclei rather than just one nucleus. In each molecular orbital, both large and small sets of orbital appear and they are mixed in the ratio that gives the lowest energy. The combination of a large orbital and a small orbital is essentially equivalent to an orbital of intermediate size. The result orbital is a size that best fit for the molecular environment since it is obtained from minimizing the energy. The advantage of this procedure is that the mixing coefficients in the molecular orbitals appear in a linear function. This simple dodge is equivalent to scaling the single minimal basis set orbitals. The minimum basis set can scaled not only the valence orbitals of the minimal basis set (split valence basis set), but also all the orbitals of the minimal basis set (double zeta basis sets).

### a) Split the Valence Orbitals (Split Valence Basis Sets)

The split valence basis sets mean that each valence orbital is spited into two parts, an inner shell and an outer shell. For example, the 3-21G basis set is referred to basis function of the inner shell represented by two Gaussian functions and that of the outer shell represented by one Gaussian function The core orbitals are represented by one basis function and each function composes of three Gaussian functions. The purpose of

splitting the valence shell is to give the SCF algorithm more flexibility in adjusting the contributions of the basis function to the molecular orbitals, achieving a more realistic simulated electron distribution.

### b) Split all Orbitals (Double Zeta Basis Sets)

Double zeta basis set is a member of minimum basis set replaced by two functions. In this way both core and valence orbitals are scaled in size. For some heavier atoms, double zeta basis sets may have slightly less than double the number of minimum basis set orbitals. For example, some double zeta basis sets for the atoms Ga-Br have 7 rather than 8 *s* basis functions, and 5 rather than 6 *p* basis functions.

The term "*double zeta*" arises from the fact that the exponent in a STO is often referred by the Greek letter "*zeta*". Since it takes two orbitals with different exponents, it is called "*double zeta*". The minimum basis set is "*single zeta*". The normal abbreviation for a double zeta basis set is DZ. It is also quite common to use split valence basis sets where the valence orbitals are spitted into three functions. Basis sets where this is done for all functions are called triple zeta functions and referred to as TZ, TZP, TZ2P etc.

### 2.4.3 Polarized Basis Sets

In the discussion on the scaling of the hydrogen orbitals in the $H_2$ molecule, it is argued that the orbital on one atom in the molecule becomes smaller because of the attraction of the other nucleus. However, it is also clear that the influence of the other nucleus may distort or polarize the electron density near the nucleus. This problem desires orbitals that have more flexible shapes in a molecule than the *s, p, d*, etc., shapes in the free atoms. This is best accomplished by add basis functions of higher angular momentum quantum number. Thus, the spherical *1s* orbital on hydrogen is distorted by mixing in an orbital with *p* symmetry. The positive lobe at one side increases the value of the orbital while the negative lobe at the other side decreases the orbital. The orbital has overall "moved" sideways. It has been polarized. Similarly, the *p* orbital can polarize if it mixes in an orbital of *d* symmetry. These additional basis functions are called polarization functions. The polarization functions are added to the 6-31G basis set as follows:

6-31G* added a set of d orbitals to the atoms in the first and second rows .

6-31G** added a set of d orbitals to the atoms in the first and second rows and a set of $p$ functions to hydrogen.

The nomenclature above is slowly being replaced. The 6-31G* is called 6-31G(d), while the 6-31G** is called 6-31G(d,p). This new nomenclature allows the possibility of adding several polarization functions. Thus 6-31G (3df,pd) added 3 $d$-type GTOs and 1 $f$-type GTO and added 1 $p$-type and 1 $d$-type function to H.

### 2.4.4 Diffuse Function Basis Sets

In some cases the normal basis functions are not adequate. This is particular the case in excited states and in anions where the electronic density is spread out more over the molecule. This model has correctly by using some basis functions which themselves are more spread out. This means that small exponents are added to GTOs. These additional basis functions are called diffuse functions. The diffuse functions added to the 6-31G basis set as follows:

6-31+G added a set of diffuse $s$ and $p$ orbitals to the atoms in the first and second rows.

Diffuse functions can be added along with polarization functions also. Some examples of these functions are 6-31+G*, 6-31++G*, 6-31+G** and 6-31++G** basis sets.

## 2.5 Density Functional Theory (DFT)

The ab initio methods described The basis for Density Functional Theory (DFT) is the proof by Hohenberg and Kohn that the ground-state electronic energy is determined completely by the electron density p, see Appendix B for details. In other words, there exists a one-to-one correspondence between the electron density of a system and the energy. The significance of this is perhaps best illustrated by comparing to the wave function approach. A wave function for an $N$-electron system contains $3N$ coordinates, three for each electron (four if spin is included). The electron density is the square of the

wave function, integrated over N-1 electron coordinates, this only depends on three coordinates, independently of the number of electrons. While the complexity of a wave function increases with the number of electrons, the electron density has the same number of variables, independently of the system size. The "only" problem is that although it has been proven that each different density yields a different ground-state energy, the functional connection these two quantities is not known. The goal of DFT methods is to design functionals connecting the electron density with the energy.

The foundation for the use of DFT methods in computational chemistry was the introduction of orbitals by Kohn and Sham. The basic idea in the Kohn and Sham (KS) formalism is splitting the kinetic energy functional into two parts, one of which can be calculated exactly, and a small correction term.

The key to Kohn-Sham thoey is thus the calculation of the kinetic energy under the assumption of non-interacting electrons. In reality the electrons are interacting, and equation (2.39) does not provide the total kinetic energy. The remaining kinetic energy is absorbed into an exchange – correlation term, and a general DFT energy expression can be written as

$$E_{DFT}[p] \; = \; T_S[p] + E_{ne}[p] + J[p] + E_{xc}[p] \tag{2.22}$$

By equating $E_{DFT}$ to the exact energy $E_{xc}$, it is the part which remains after subtraction of the non-interacting kinetic energy, and the $E_{ne}$ and $J$ potential energy terms:

$$E_{xc}[p] \; = \; (T[p] - T_S[p]) + (E_{ee}[p] - J[p]) \tag{2.23}$$

The first parenthesis in equation (2.44) may be considered the kinetic correlation energy, while the second contains both exchange and potential correlation energy [17].

**2.6 Transition State Theory and Statistical Mechanics**

*Transition state theory* (TST) assumes that a reaction proceeded from one energy minimum to another *via* an intermediate maximum. The *transition state* is the configuration which divides the reactant and product parts of surface. For example, a molecule which has reached the transition state is continuing to product. The geometrical configuration of the energy maximum is called the *transition structure*. Within standard TST, the transition state and transition structure are identical, but this is not necessarily for more refined models. The direction of reaction coordinate is started from the reactant to product along a path where the energies are as low as possible and the TS is the point where the energy has a maximum. In the multidimensional case, TS is a first-order point on the potential energy surface as a maximum in the reaction coordinate direction and a minimum along all other coordinates, shown in Figure 2.1.
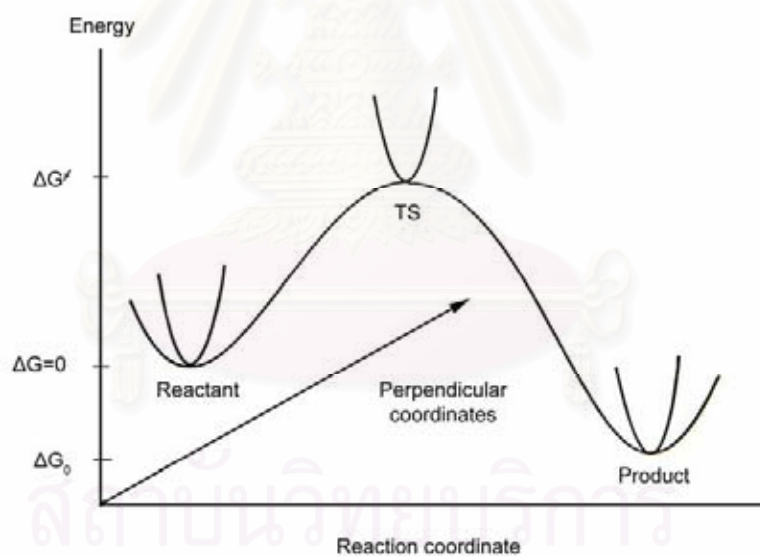


**Figure 2.1** Schematic illustration of reaction path *[16]*.

Transition state theory assumes equilibrium energy distribution among all possible quantum states at all points along the reaction coordinates. The probability of finding a molecular in a given quantum state is proportional to $e^{-\Delta E/k_B T}$, which is

Boltzman distribution. Assuming that the molecule at the TS is in equilibrium with the reactant, the macroscopic rate constant can be expressed as:

$$k = \frac{k_B T e^{-\Delta G^{\neq}/RT}}{h}$$ (2.24)

in which $\Delta G^{\neq}$ is the Gibbs free energy difference between the TS and reactant, T is absolute temperature and $k_B$ is Boltzmann's constant. It is clear that if the free energy of the reactant and TS can be calculated, the reactant rate follows trivially. The equilibrium constant for a reaction can be calculated from the free energy difference between the reactant and product.

$$K_{eq} = e^{-\Delta G_0/RT}$$ (2.25)

The Gibbs free energy is given in terms of the enthalpy and entropy, $G = H - TS$. The enthalpy and entropy for a macroscopic ensemble of particles maybe calculated from properties of the individual molecules by means of statistical mechanics.
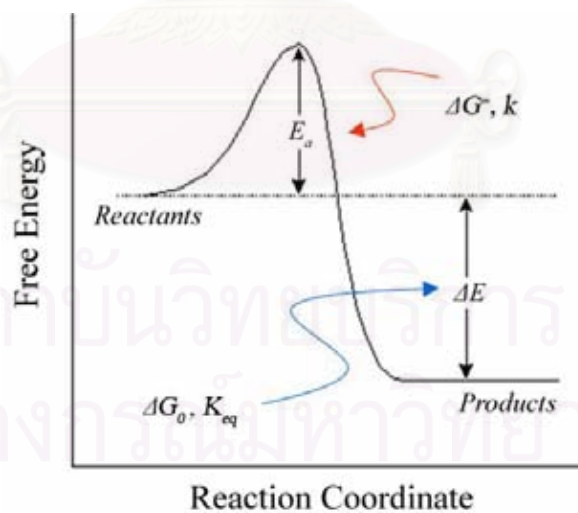


**Figure 2.2** The difference between rate constant ($k$) and equilibrium constant ($K$) [16].

**2.7 The Conductor-Like Polarizable Continuum Model (CPCM)**

Many chemical and biological reactions occur in water, where the polar and ionic processes are much more favorable than in the gas phase. Many efforts have been devoted to the development of methods to compute reaction barriers and energetics occurring in condensed phases with experimental accuracy. Effective explicit water models become available for the description of chemical systems in liquid solution.

Dielectric continuum theories are now widely used to describe hydration in conjunction with quantum mechanical calculations due to the relatively low cost of the calculation. CPCM *[18-20]* and PCM are two of many successful solvation models. In their approaches, the solute interacts with the solvent represented by a dielectric continuum model. The solute molecule is embedded into a cavity surrounded by a dielectric continuum of permittivity. The accuracy of continuum solvation models depends on several factors; the most important one is the use of proper boundary conditions on the surface of the cavity containing the solute CPCM *[18-20]* and PCM define the cavities as envelopes of spheres centered on atoms or atomic groups: a number of cavity models have been suggested. Inside the cavity the dielectric constant is the same as in vacuo, outside it takes the value of the desired solvent. Once the cavity has been defined, the surface is smoothly mapped by small regions, called tesserae. Each tessera is characterized by the position of its center, its area, and the electrostatic vector normal to the surface passing through its center. Recently, the CPCM *[18-20]* method has been improved and extended in GAUSSIAN 03 *[21]* Program so that the cavity can be selected in a number of different ways. In CPCM, *[18-20]* the solvation free energy can be expressed:

$$\Delta G_{solv} = \Delta G_{el} + \Delta G_{cav} + \Delta G_{dis} + \Delta G_{rep} +$$
$$RTIn\left(\frac{q_{rot,g}q_{vib,q}}{q_{rot,s}q_{vib,s}}\right) - RTIn\left(\frac{n_{solute,g}\Lambda_{solute,g}}{n_{solute,s}\Lambda_{solute,s}}\right) + P\Delta V \qquad (2.26)$$

$\Delta G_{el}$ is the electrostatic component of $\Delta G_{solv}$. The $G_{el}$ term is calculated using the CPCM *[18-20]* self-consistent reaction field (SCRF) method. The cavitation term, $\Delta G_{cav}$, is calculated with the expression derived by Pierotti from the hard sphere theory and

adapted to the case of nonspherical cavities. The dispersion and repulsion terms, $\Delta G_{\text{dis}}$ and $\Delta G_{\text{rep}}$, are computed following Floris and Tomasi's procedure, with the parameters proposed by Callet and Claverie *[22]*. The $q_{\text{rot}}$, g, $q_{\text{vib}}$,g, $q_{\text{rot}}$, s, and $q_{\text{vib}}$, s are denoted the microscopic partition functions for rotational and vibrational states of the solute in the gas phase and in solution, respectively; *n* solute, g and *n* solute, s are the numeral densities of solute; and solute, g and solute, s are the momentum partition functions.

## 2.8 Frontier molecular orbitals (HOMO and LUMO)

HOMO and LUMO are acronyms for highest occupied molecular orbital and lowest unoccupied molecular orbital, respectively. The difference of the energies of the HOMO and LUMO, termed the band gap can sometimes serve as a measure of the excitability of the molecule: the smaller the energy, the more easily it will be excited.

Those who are already familiar with inorganic semiconductors see that the HOMO level is to organic semiconductors what the valence band is to inorganic semiconductors. The same analogy exists between the LUMO level and the conduction band. The energy difference between the HOMO and LUMO level is regarded as band gap energy.

When the molecule forms a dimer or an aggregate, the proximity of the orbitals of the different molecules induce a splitting of the HOMO and LUMO energy levels. This splitting produces vibrational sublevels which each have their own energy, slightly different from one another. There are as many vibrational sublevels as there are molecules that interact together. When there are enough molecules influencing each other (e.g. in an aggregate), there are so many sublevels that we no longer perceive their discrete nature: they form a continuum. We no longer consider energy levels, but energy bands *[23]*.

# CHAPTER III

# DETAILS OF THE CALCULATIONS

## 3.1 Methods of calculations

Geometries of aldehydes, intermediates, transition states and products in hydrophosphonylation were optimized using density functional theory (DFT) method. *[24,25]* DFT calculations have been performed with the Becke's three-parameter exchange functional *[26-27]* with the Lee-Yang-Parr correlation functional (B3LYP) *[28]* follow mechanism as below:
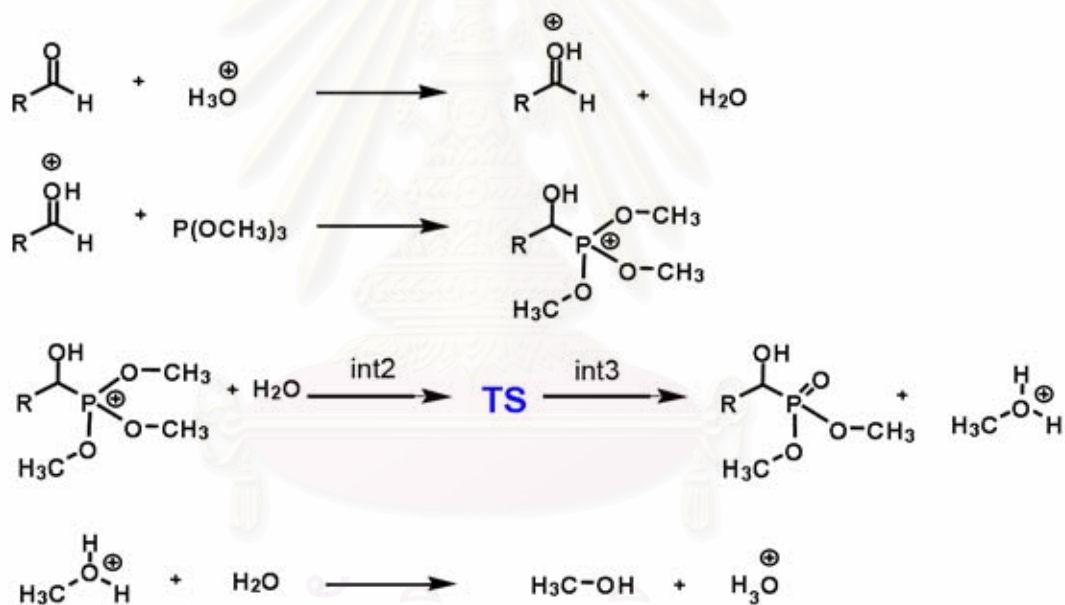


**Figure 3.1** The mechanism of aldehyde conversions to α-hydroxy phosphonates in acid-catalyzed system that was proposed in this work.

### 3.1.1 Gas phase

All roughly geometry for acetaldehyde reactant have been carried out using the computations at the B3LYP/6-31G(d). Then, to calculate more optimized

structures for this reactant by B3LYP/6-311+G(d,p) level and in the same level, optimized geometry for *i*-propyl aldehyde reactants were calculated.

All minima and transition states were confirmed by real and single imaginary vibrational frequencies, respectively.

### 3.1.2 Aqueous phase

The solvent effect was investigated by single-point computations on the B3LYP/6-311+G(d,p)-optimized gas-phase structures using the conductor-like polarizable continuum model (CPCM) *[18-20]*.

The standard enthalpy $\Delta H^O$ and Gibbs free energy changes $\Delta G^O$ of conversion reactions of this system have been derived from the frequency calculations. Each reaction entropy $\Delta S^O$ was calculated using a thermodynamic relation of $\Delta S^O = (\Delta H^O - \Delta G^O)/T$. The rate constant $k(T)$ and equilibrium constant $K$ derived from transition state theory was computed from activation free energy, $\Delta^{\ddagger}G^O$ by

$$k(T) = \frac{k_B T}{hc^o} \exp(-\Delta^{\ddagger}G^O/RT) \tag{3.1}$$

and

$$K = (-\Delta^{\ddagger}G^O/RT) \tag{3.2}$$

Where concentration factor, $c^o$ of unity is used, $k_B$ is Boltzmann's constant, $h$ is Plank's constant, $T$ is the absolute temperature and $R$ is gas constant. The above formula was employed to compute the reaction rate constants for corresponding activation free energies.
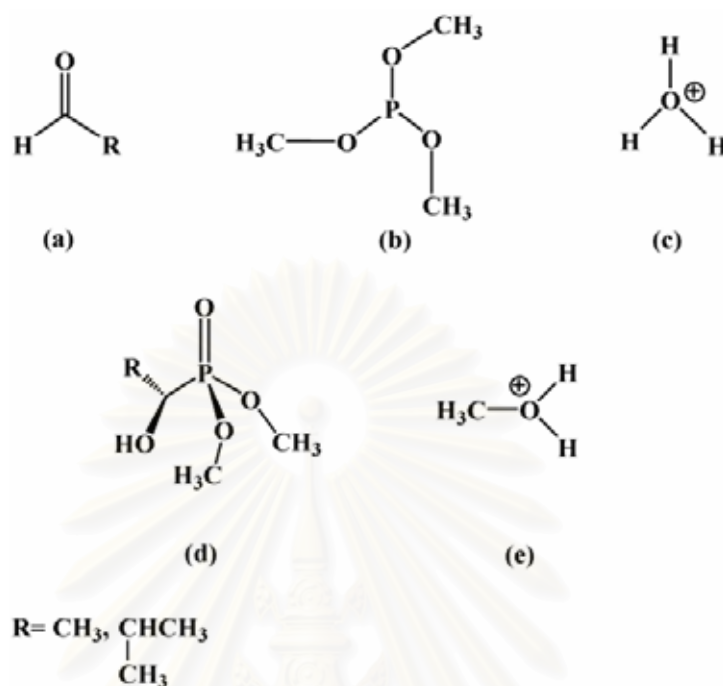
**Figure 3.2** Structures of aldehydes (a), trimethylphosphite (b), hydronium ion (c), α-hydroxy phosphonates (d) and protonated methanal (e).

All calculations were performed with the GAUSSIAN 03 *[21]* program. The MOLDEN 4.2 program *[29]* was utilized to display the molecular structure, monitor the geometrical parameters and observe the molecular geometry convergence *via* the Gaussian output files. The molecular graphics of all related species were generated with the MOLEKEL 4.3 program *[30]*.

# CHAPTER IV

# RESULTS AND DISCUSSION

The B3LYP/6-311+G(d,p) optimized structures of aldehydes, their intermediates, transition states, α-hydroxy phosphonate product and all related species in acetaldehyde and *i*-propyl aldehyde conversion reactions were obtained. Mechanism of the acetaldehyde (ald) and *i*-propyl aldehyde (ald_2) conversions to their corresponding α-hydroxy phosphonates comprise of six reaction steps:

$$ald(\_2) \quad + \quad H_3O^+ \quad \rightarrow \quad ald(\_2).H^+ \quad + H_2O \qquad (1)$$

$$ald(\_2).H^+ + \quad tmp \quad \rightarrow \quad int1(\_2) \qquad\qquad\qquad (2)$$

$$int1(\_2) \quad + \quad H_2O \quad \rightarrow \quad int2(\_2) \qquad\qquad\qquad (3)$$

$$int2(\_2) \quad \rightarrow \quad TS(\_2) \quad \rightarrow \quad int3(\_2) \qquad\qquad (4)$$

$$int3(\_2) \quad \rightarrow \quad ahp(\_2) \quad + \quad MeOH_2^+ \qquad\qquad (5)$$

$$MeOH_2^+ \quad + \quad H_2O \quad \rightarrow \quad MeOH \quad + \quad H_3O^+ \qquad (6)$$
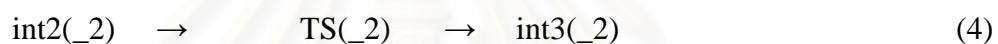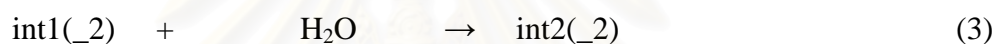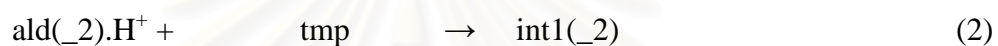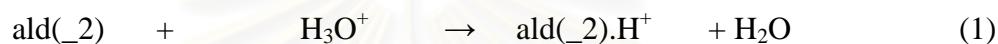
The first reaction, aldehyde is protonated by catalytic hydronium ion to prepare the protonated aldehyde which reacts with trimethyl phosphonate (tmp) to produce species int1, eqs. (1) and (2). The third reaction step is a hydration reaction of int1 producing species int2. The fourth reaction is a rate-determining step of which rate constant is calculated using transition state theory. The fifth reaction affords the alpha hydroxy phosphonate (ahp or ahp_2). The last step is the releasing process for freeing a molecule of hydronium ion.

## 4.1 Acetaldehyde conversion reactions

The reactions based on eqs (3) to (5) for the acetaldehyde conversion to α-hydroxy phosphonate (ahp) is shown in Figure 4.1. The changes of bond distances P-O1, P-O2 and P-O3 as defined in Figure 4.1 for species int1, int2, TS, int3 and product ahp are shown in Figures 4.2 and 4.3 based on the B3LYP/6-31G(d) and B3LYP/6-311+G(d,p) levels of theory, respectively. The changes of these bond distances computed at two different levels of theory are very similar. Moreover,

geometrical data for the species int1, int2, TS, int3 and product ahp, based on the B3LYP/6-31G(d) and B3LYP/6-311+G(d,p) calculations are shown in Tables 4.1 and 4.2, respectively. Overall reaction presented as hydrophosphonylation cycle of acetaldehyde conversion is given in Figure 4.4.

Relative energetic profiles based on the B3LYP/6-31G(d) and B3LYP/6-311+G(d,p) calculations of the acetaldehyde conversion reactions in gas phase are shown in Figures 4.5 and 4.6, respectively. In aqueous phase, its relative energetic profile based on the B3LYP/6-311+G(d,p) calculation as showed in Figure 4.7 is very different compared to the gas phase potential.

Rate and equilibrium constants, energetics and thermodynamic properties of acetaldehyde conversion, computed at the B3LYP/6-31G(d) and B3LYP/6-311+G(d,p) levels in gas phase and at the B3LYP/6-311+G(d,p) level in aqueous pahse are shown in Tables 4.3 and 4.4, respectively.

These two tables show that whether in gas phase or aqueous phase the reaction step *via* the transition state is rate-determining step of their overall reactions.
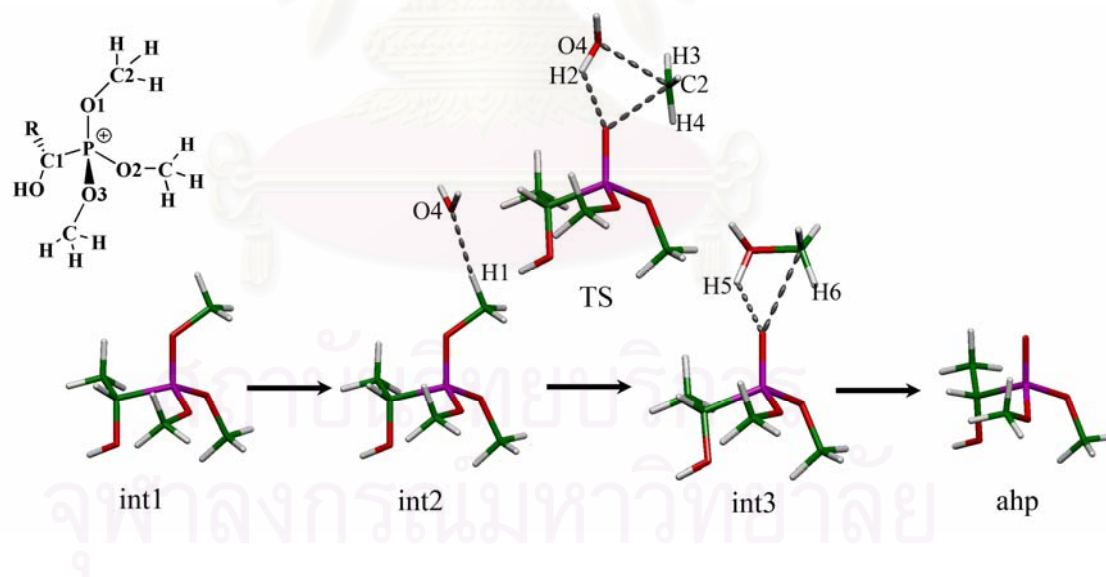


**Figure 4.1** Reaction Mechanism of acetaldehyde conversion.

**Figure 4.2** Plot of bond distances (Å) P-O1, P-O2 and P-O3 of involved species in acetaldehyde conversion system.



**Figure 4.3** Plot of bond distances (Å) P-O1, P-O2 and P-O3 of involved species in acetaldehyde conversion system.

**Table 4.1** Geometrical data based on the B3LYP/6-31G(d) calculations of intermediates, transition state and product in acetaldehyde conversion system in gas phase

| Parameter/Conformer | int1 | int2 | TS | int3 | ahp |
|---|---|---|---|---|---|
| Bond distance (Å) | | | | | |
| H1-O4 | - | 2.1284 | - | - | - |
| H2-O1 | - | - | 1.8173 | - | - |
| C2-O4 | - | - | 2.2809 | - | - |
| O1-C2 | 1.4681 | 1.4771 | 2.2504 | 2.5409 | - |
| O1-H5 | - | - | - | 1.7565 | - |
| O1-P | 1.5687 | 1.5625 | 1.5239 | 1.4967 | 1.4821 |
| P-O2 | 1.5691 | 1.5703 | 1.5918 | 1.5966 | 1.6062 |
| P-O3 | 1.5791 | 1.5775 | 1.5892 | 1.6005 | 1.6224 |
| P-C1 | 1.8355 | 1.8353 | 1.8442 | 1.8457 | 1.8476 |
| Bond Angle  (Degree) | | | | | |
| C2-O1-P | 124.71 | 124.85 | - | - | - |
| O1-P-O2 | 107.37 | 108.10 | 107.78 | 110.44 | 114.38 |
| O1-P-O3 | 113.78 | 113.99 | 115.42 | 115.90 | 116.14 |
| O1-P-C1 | 104.12 | 104.29 | 110.07 | 110.71 | 111.47 |

[a] Atomic numbers are shown in Figure 4.1.

**Table 4.2** Geometrical data based on the B3LYP/6-311+G(d,p) calculations of intermediates, transition state and product in acetaldehyde conversion system in gas phase

| Parameter/Conformer | int1 | int2 | TS | int3 | ahp |
|---|---|---|---|---|---|
| Bond distance (Å) | | | | | |
| H1-O4 | - | 2.1876 | - | - | - |
| H2-O1 | - | - | 1.8079 | - | - |
| C2-O4 | - | - | 2.3099 | - | - |
| O1-C2 | 1.4697 | 1.4781 | 2.2838 | 2.6453 | |
| O1-H5 | - | - | - | 1.6444 | - |
| O1-P | 1.5638 | 1.5586 | 1.5198 | 1.5106 | 1.4797 |
| P-O2 | 1.5638 | 1.5643 | 1.5883 | 1.5928 | 1.6002 |
| P-O3 | 1.5703 | 1.5732 | 1.5846 | 1.5885 | 1.6186 |
| P-C1 | 1.8355 | 1.8351 | 1.8448 | 1.8467 | 1.8482 |
| Bond Angle  (Degree) | | | | | |
| C2-O1-P | 126.61 | 126.56 | - | - | - |
| O1-P-O2 | 107.46 | 108.08 | 107.62 | 110.44 | 114.53 |
| O1-P-O3 | 113.64 | 113.74 | 115.21 | 115.90 | 115.70 |
| O1-P-C1 | 104.07 | 104.25 | 110.17 | 110.71 | 110.99 |

[a] Atomic numbers are shown in Figure 4.1.
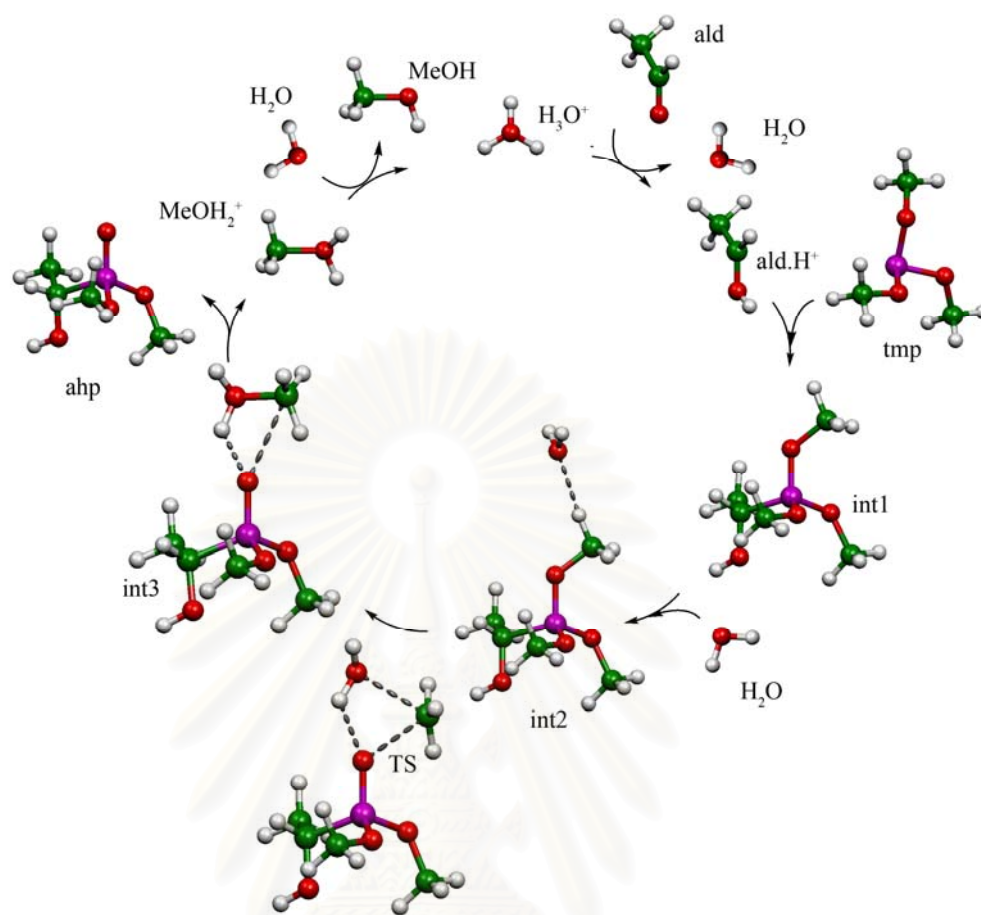
**Figure 4.4** Hydrophosphonylation cycle of acetaldehyde conversion.

**Figure 4.5** Relative energetic profile based on the B3LYP/6-31G(d) calculations of acetaldehyde conversion reaction in gas phase.



**Figure 4.6** Relative energetic profile based on the B3LYP/6-311+G(d,p) calculations of acetaldehyde conversion reaction in gas phase.

**Figure 4.7** Relative energetic profile based on the B3LYP6-311+G(d,p) calculations of acetaldehyde conversion reaction in aqueous phase.

**Table 4.3** Rate, equilibrium constants, energetics and thermodynamic properties of aldehyde conversion to α-hydroxy phosphonate in acetaldehyde system in gas phase

| Reactions | $\Delta^{\ddagger}E^{\,a,\,b}$ | $\Delta^{\ddagger}G^{\,a}$ | $k_{298}^{\,c}$ | $\Delta E^{\,a,\,b}$ | $\Delta H_{298}^{\,a,b}$ | $\Delta G_{298}^{\,a,b}$ | $K_{298}$ |
|---|---|---|---|---|---|---|---|
| **B3LYP/6-31+G(d)** | | | | | | | |
| ald+$H_3O^+\rightarrow$ ald.$H^+$+$H_2O$ | - | - | - | -16.78 | -16.74 | -17.00 | $2.90\times10^{+12}$ |
| ald.$H^+$+ tmp$\rightarrow$ int1 | - | - | - | -52.20 | -52.61 | -40.05 | $2.29\times10^{+29}$ |
| int1+$H_2O\rightarrow$ int2 | - | - | - | -6.30 | -6.08 | 0.02 | $9.62\times10^{-1}$ |
| int2 $\rightarrow$ TS $\rightarrow$ int3 | 48.18 | 50.89 | $3.07\times10^{-25}$ | 37.59 | 33.84 | 44.41 | $2.80\times10^{-33}$ |
| int3 $\rightarrow$ ahp + $MeOH_2^+$ | - | - | - | 9.80 | 12.36 | -4.68 | $2.69\times10^{+3}$ |
| **B3LYP/6-311+G(d,p)** | | | | | | | |
| ald+$H_3O^+\rightarrow$ ald.$H^+$+$H_2O$ | - | - | - | -20.21 | -20.20 | -20.42 | $9.34\times10^{+14}$ |
| ald.$H^+$+ tmp$\rightarrow$ int1 | - | - | - | -47.91 | -48.26 | -36.10 | $2.90\times10^{+26}$ |
| int1 + $H_2O\rightarrow$ int2 | - | - | - | -5.11 | -4.88 | 1.26 | $1.10\times10^{-1}$ |
| int2 $\rightarrow$ TS $\rightarrow$ int3 | 48.81 | 51.33 | $1.46\times10^{-25}$ | 14.37 | 11.83 | 18.43 | $3.10\times10^{-14}$ |
| int3 $\rightarrow$ ahp + $MeOH_2^+$ | - | - | - | 34.38 | 35.74 | 22.73 | $2.16\times10^{-17}$ |

[a] In kcal mol$^{-1}$.
[b] Total energy with zero-point energy corrections.
[c] In s$^{-1}$.

**Table 4.4** Rate, equilibrium constants, energetics and thermodynamic properties of aldehyde conversion to α-hydroxy phosphonate in acetaldehyde system in aqueous phase

| Reactions | $\Delta^{\ddagger}E^{\,a,\,b}$ | $\Delta\Delta^{\ddagger}G^{\,b}$ | $k_{298}^{\,c}$ | $\Delta E^{\,a,\,b}$ | $\Delta\Delta G_{298}^{\,a,b}$ | $K_{298}$ |
|---|---|---|---|---|---|---|
| ald+$H_3O^+\rightarrow$ ald.$H^+$+$H_2O$ | - | - | - | 14.05 | 14.34 | $3.10\times10^{-11}$ |
| ald.$H^+$+ tmp$\rightarrow$ int1 | - | - | - | -23.02 | -21.57 | $6.52\times10^{+15}$ |
| int1 +$H_2O\rightarrow$ int2 | - | - | - | 4.35 | 5.40 | $1.10\times10^{-4}$ |
| int2 $\rightarrow$ TS $\rightarrow$ int3 | 44.99 | 45.09 | $5.43\times10^{-21}$ | -7.38 | -8.48 | $1.65\times10^{+6}$ |
| int3 $\rightarrow$ ahp + $MeOH_2^+$ | - | - | - | -4.99 | -5.66 | $1.41\times10^{+4}$ |

[a] In kcal mol$^{-1}$.
[b] Total energy with non-zero point energy corrections.
[c] In s$^{-1}$.

### 4.2 *i*-propyl aldehyde conversion reactions

The reactions based on eqs (3) to (5) for the *i*-propyl aldehyde conversion to *i*-propyl (ahp_2) α-hydroxy phosphonate is shown in Figure 4.8. The changes of bond distances P-O1, P-O2 and P-O3 based on the B3LYP/6-311+G(d,p) computation for species int1_2, int2_2, TS_2, int3_2 and product ahp_2 is shown in Figure 4.9. Geometrical data for the species int1_2, int2_2, TS_2, int3_2 and product ahp_2, obtained from the B3LYP/6-311+G(d,p) calculation are lised in Table 4.5. Overall reaction presented as hydrophosphonylation cycle of *i*-propyl aldehyde conversion is given in Figure 4.10.

Relative energetic profiles computed at the B3LYP/6-311+G(d,p) level of theory of the *i*-propyl aldehyde conversion reactions in gas phase and aqueous phase are shown in Figures 4.11 and 4.12, respectively.

Rate and equilibrium constants, energetics and thermodynamic properties of acetaldehyde conversion, computed at the B3LYP/6-311+G(d,p) level in gas phase and aqueous phase are shown in Tables 4.6 and 4.7, respectively.

These two tables show that whether in gas phase or aqueous phase the reaction step *via* the transition state is rate-determining step of their overall reactions.
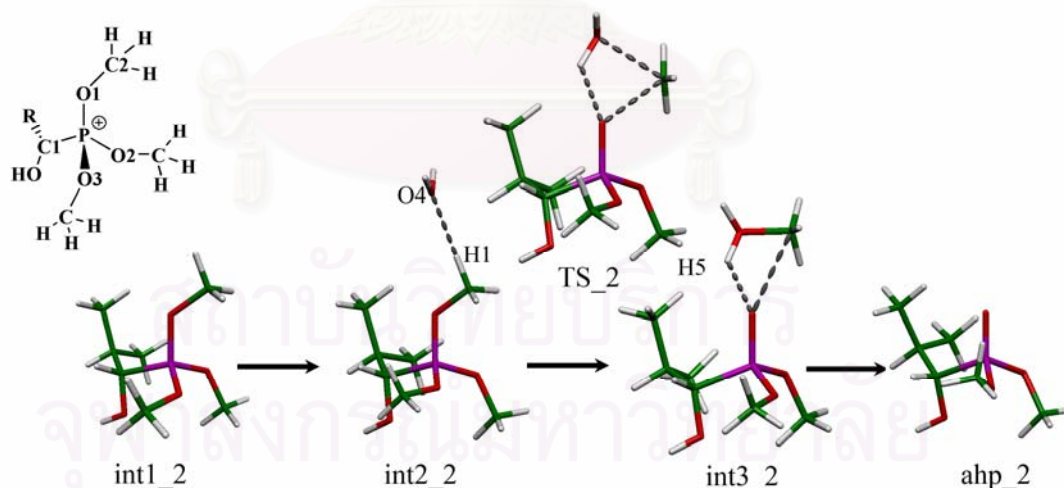


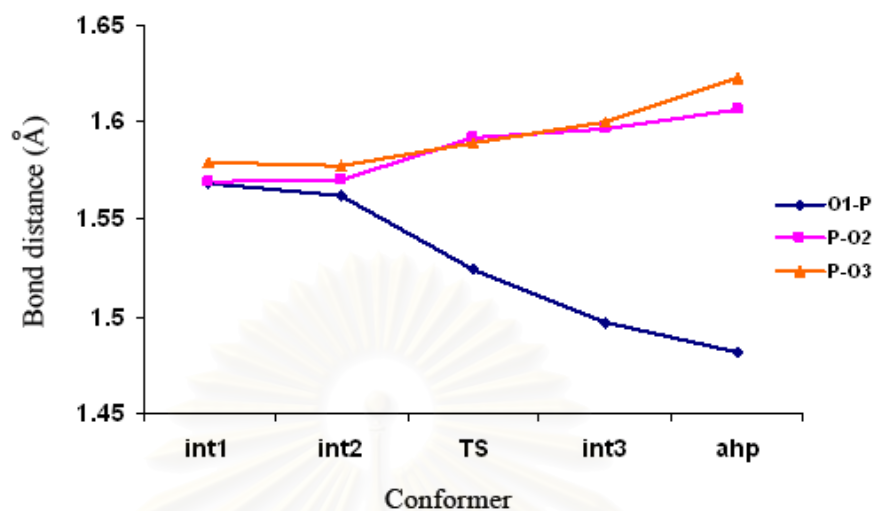**Figure 4.8** Reaction Mechanism of *i*-propyl aldehyde conversion.
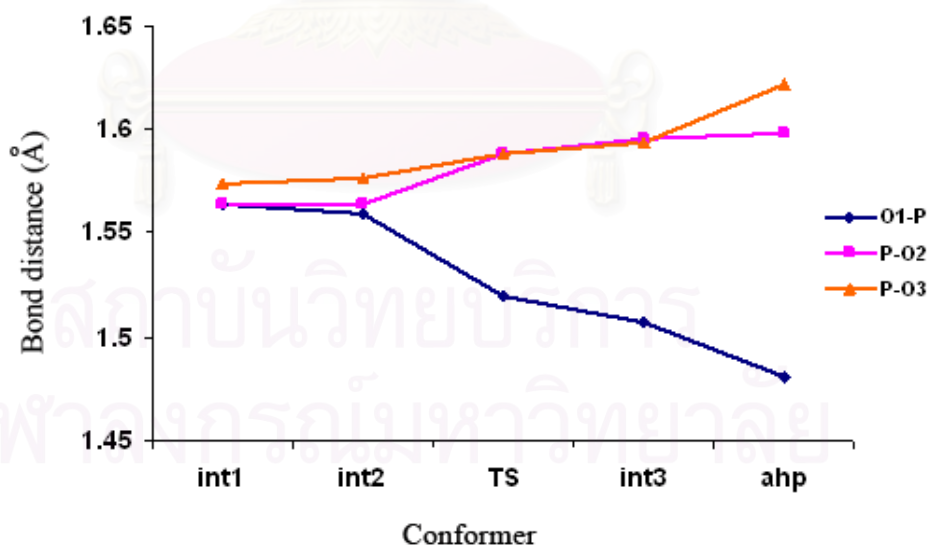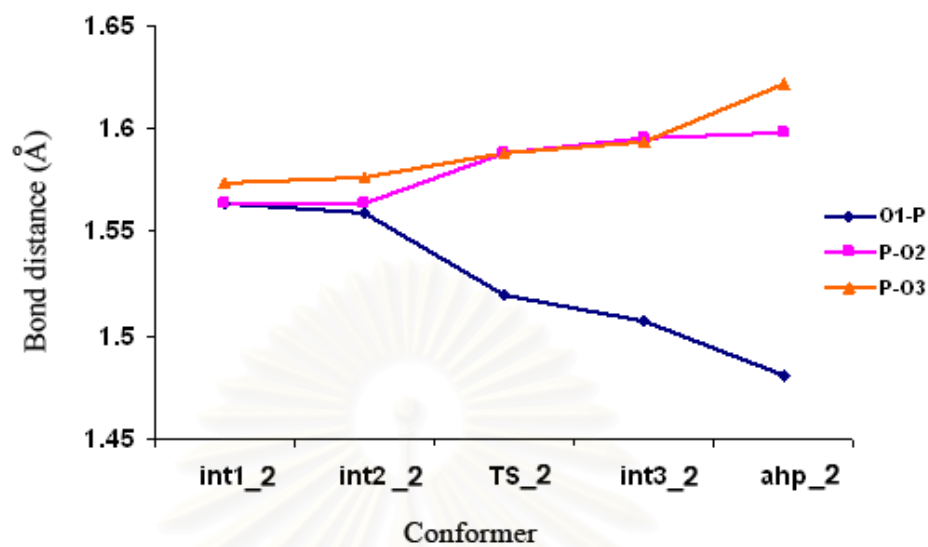
**Figure 4.9** Plot of bond distances (Ǻ) P-O1, P-O2 and P-O3 of involved species in
*i*-propyl aldehyde conversion system.

**Table 4.5** Geometrical data based on the B3LYP/6-311G(d,p) calculations of intermediates, transition state and product in *i*-propyl aldehyde conversion system in gas phase

| System/parameter [a] | int1_2 | int2_2 | TS_2 | int3_2 | ahp_2 |
|---|---|---|---|---|---|
| Bond distance (Å) | | | | | |
| H1-O4 | - | 2.1921 | - | - | - |
| H2-O1 | - | - | 1.8129 | - | - |
| C2-O4 | - | - | 2.2997 | - | - |
| O1-C2 | 1.4694 | 1.4775 | 2.2834 | 2.7077 | - |
| O1-H5 | - | - | - | 1.7278 | - |
| O1-P | 1.5644 | 1.5595 | 1.5199 | 1.5070 | 1.4807 |
| P-O2 | 1.564 | 1.5642 | 1.5884 | 1.5959 | 1.5985 |
| P-O3 | 1.5742 | 1.5769 | 1.5887 | 1.5939 | 1.6221 |
| P-C1 | 1.8417 | 1.8411 | 1.8527 | 1.8545 | 1.8552 |
| Bond Angle  (Degree) | | | | | |
| C2-O1-P | 125.97 | 125.96 | - | - | - |
| O1-P-O2 | 107.21 | 107.71 | 107.44 | 110.10 | 114.13 |
| O1-P-O3 | 112.80 | 112.99 | 114.61 | 115.15 | 115.02 |
| O1-P-C1 | 105.64 | 105.92 | 111.40 | 112.49 | 112.70 |

[a] Atomic numbers are shown in Figure 4.8.
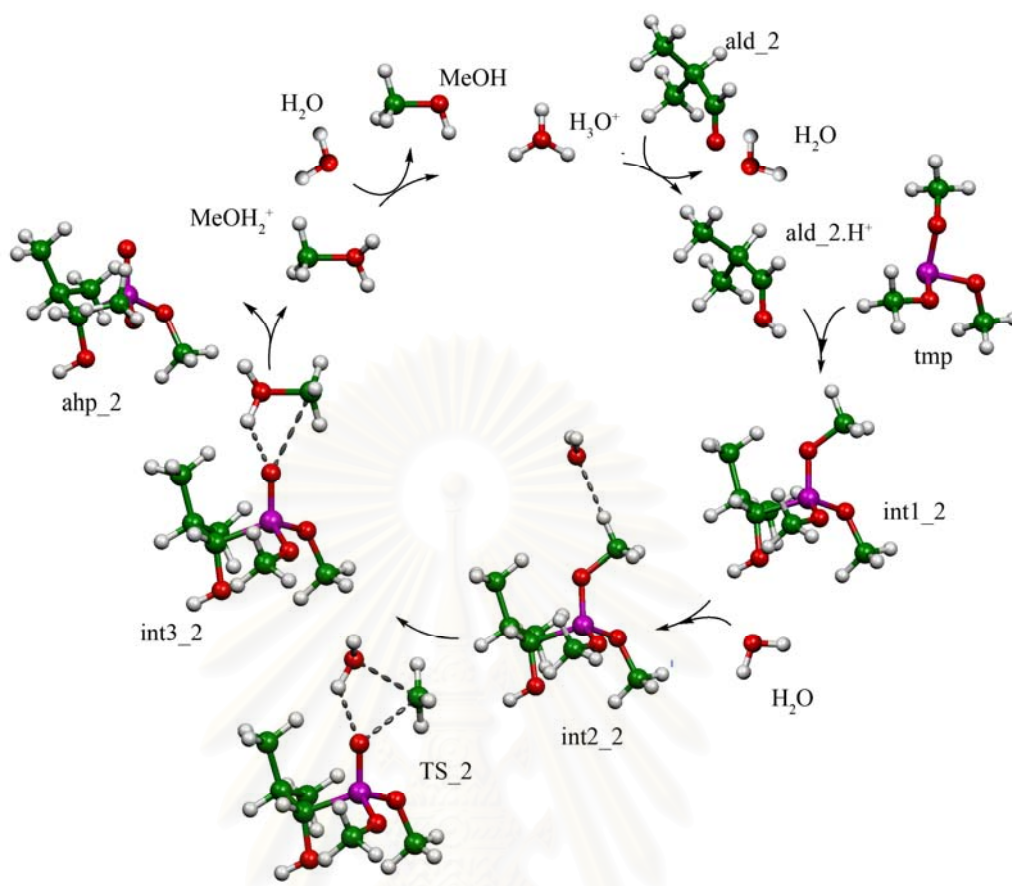
**Figure 4.10** Hydrophosphonylation cycle of *i*-propyl aldehyde conversion.
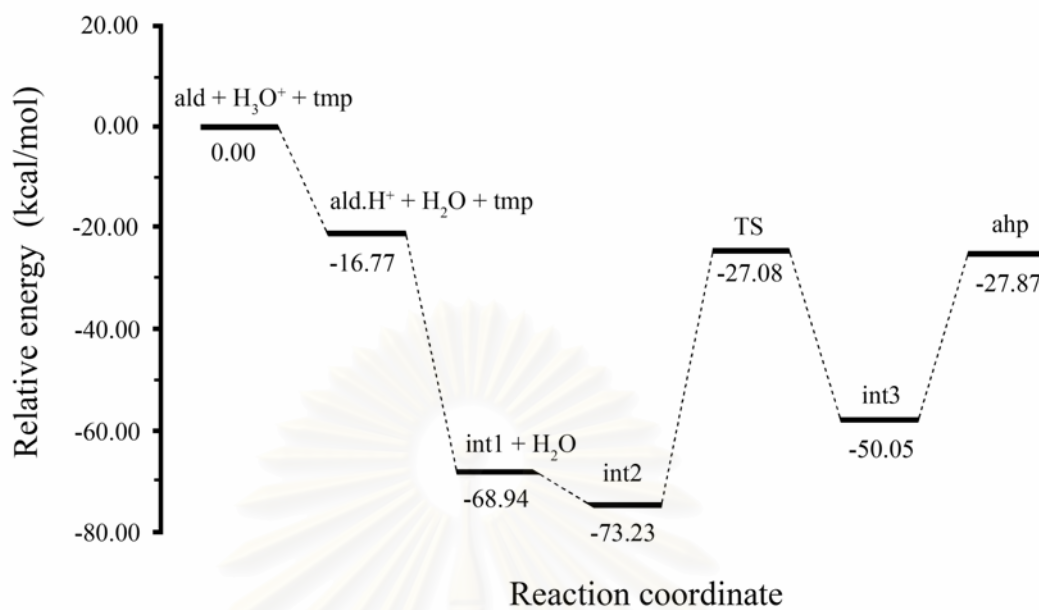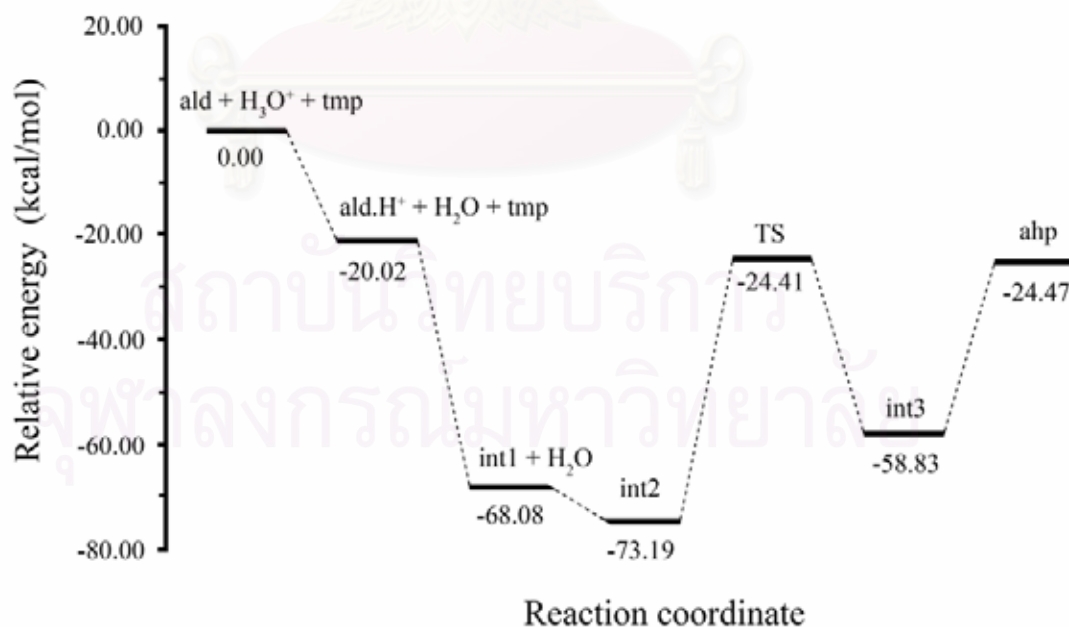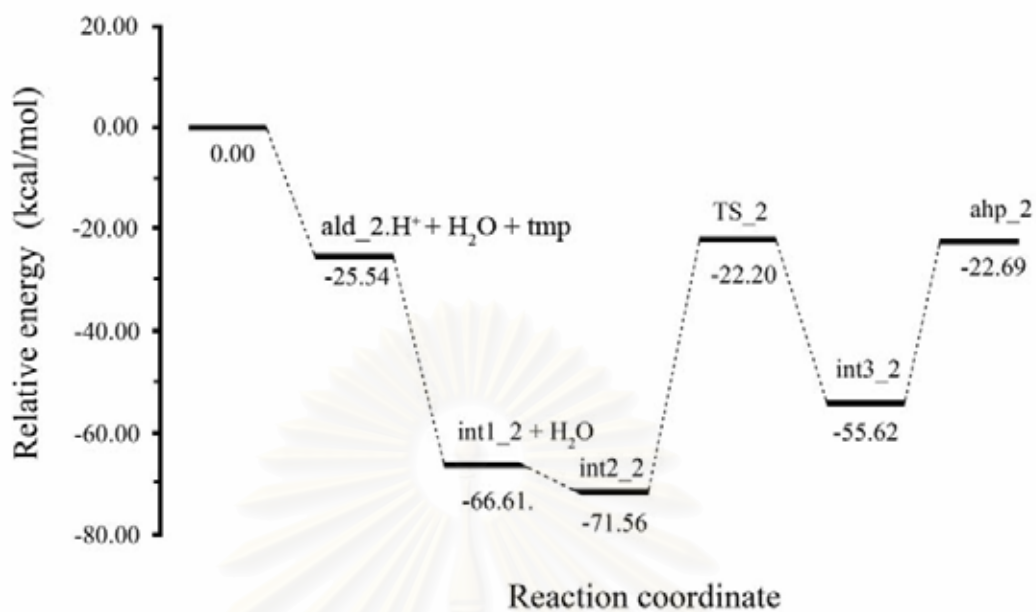
**Figure 4.11** Relative energetic profile based on the B3LYP/6-311+G(d,p) calculations of *i*-propyl aldehyde conversion reaction in gas phase.
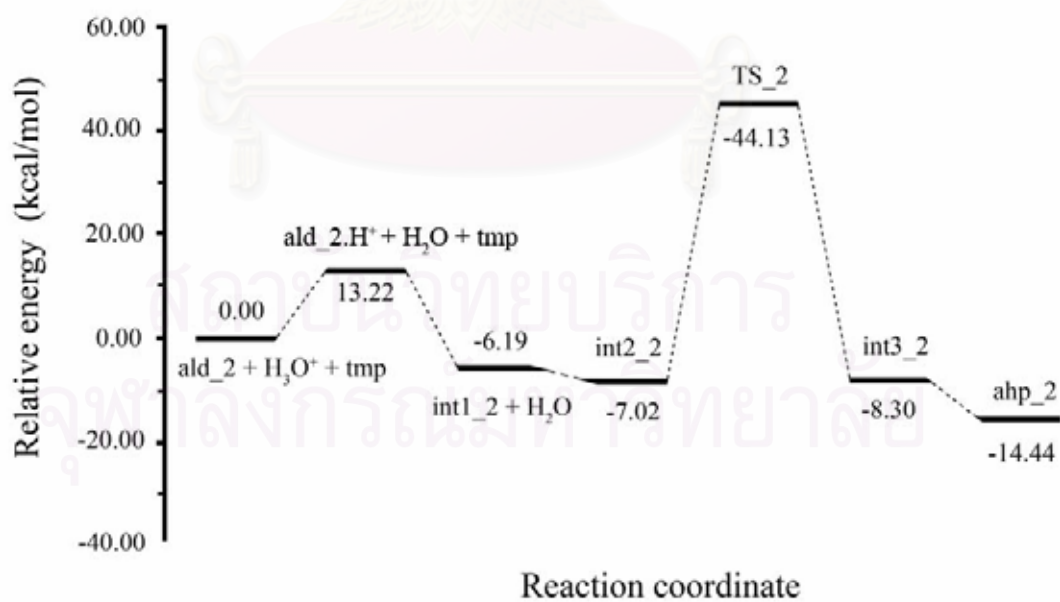


**Figure 4.12** Relative energetic profile based on the B3LYP/6-311+G(d,p) calculations of *i*-propyl aldehyde conversion reaction in aqueous phase.
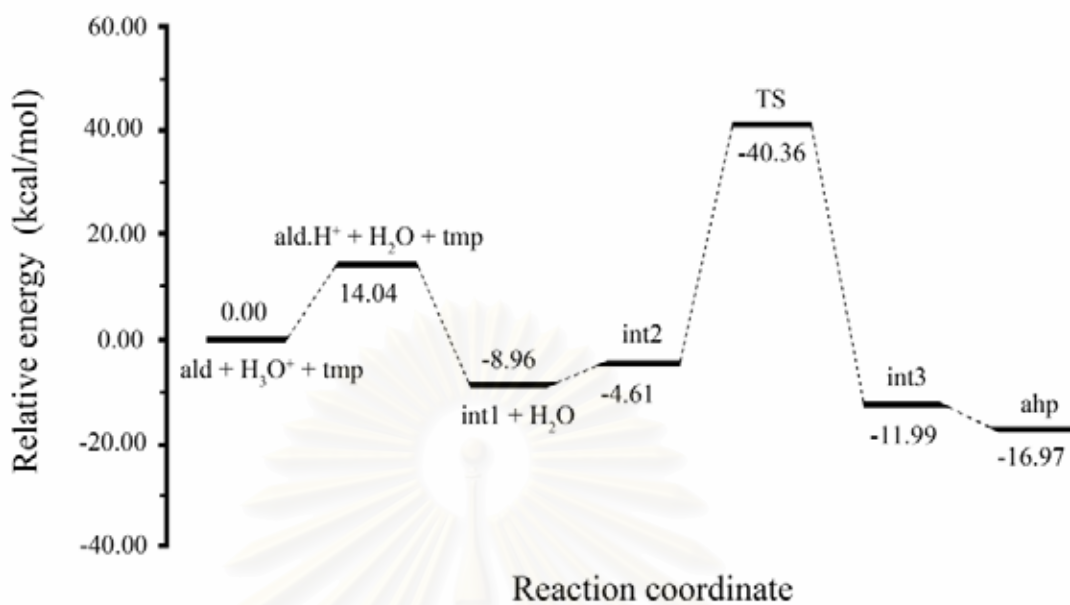
**Table 4.6** Rate, equilibrium constants, energetics and thermodynamic properties of aldehyde conversion to α-hydroxy phosphonate in *i*-propyl aldehyde system in gas phase

| Reactions | $\Delta^{\ddagger}E$ [a, b] | $\Delta^{\ddagger}G$ [a] | $k_{298}$ [c] | $\Delta E$ [a, b] | $\Delta H_{298}^{a,b}$ | $\Delta G_{298}^{a,b}$ | $K_{298}$ |
|---|---|---|---|---|---|---|---|
| ald_2 + $H_3O^+ \rightarrow$ ald_2.$H^+$ + $H_2O$ | - | - | - | -25.56 | -25.51 | -25.84 | $8.83 \times 10^{+18}$ |
| ald_2.$H^+$ + tmp$\rightarrow$ int1_2 | - | - | - | -41.09 | -41.35 | -28.49 | $7.69 \times 10^{+20}$ |
| int1_2 + $H_2O \rightarrow$ int2_2 | - | - | - | -4.96 | -4.76 | 1.44 | $8.87 \times 10^{-2}$ |
| int2_2 → TS_2 → int3_2 | 49.39 | 51.95 | $5.14 \times 10^{-26}$ | 15.95 | 13.13 | 20.71 | $6.61 \times 10^{-16}$ |
| int3_2→ ahp_2 + MeOH$_2^+$ | - | - | - | 32.94 | 34.67 | 20.44 | $1.04 \times 10^{-15}$ |

[a] In kcal mol$^{-1}$.
[b] Total energy with zero-point energy corrections.
[c] In s$^{-1}$.

**Table 4.7** Rate, equilibrium constants, energetics and thermodynamic properties of aldehyde conversion to α-hydroxy phosphonate in *i*-propyl aldehyde system in aqueous phase

| Reactions | $\Delta^{\ddagger}E$ [a, b] | $\Delta\Delta^{\ddagger}G$ [b] | $k_{298}$ [c] | $\Delta E$ [a, b] | $\Delta\Delta G_{298}^{a,b}$ | $K_{298}$ |
|---|---|---|---|---|---|---|
| ald_2 + $H_3O^+ \rightarrow$ ald_2.$H^+$+$H_2O$ | - | - | - | 13.23 | 13.61 | $1.06 \times 10^{-10}$ |
| ald_2.$H^+$ + tmp$\rightarrow$ int1_2 | - | - | - | -19.42 | -16.20 | $7.58 \times 10^{+11}$ |
| int1_2 + $H_2O \rightarrow$ int2_2 | - | - | - | -0.84 | 0.54 | $4.02 \times 10^{-1}$ |
| int2_2 → TS_2 → int3_2 | 51.19 | 50.92 | $2.93 \times 10^{-25}$ | -1.28 | -2.56 | $7.56 \times 10^{+1}$ |
| int3_2→ ahp_2 + MeOH$_2^+$ | - | - | - | -6.14 | -7.24 | $2.03 \times 10^{+5}$ |

[a] In kcal mol$^{-1}$.
[b] Total energy with non-zero point energy corrections.
[c] In s$^{-1}$.

## 4.3 Frontier molecular orbitals

The highest occupied molecular orbital (HOMO), lowest unoccupied molecular orbital (LUMO) of aldehydes ald, ald_2, protonated aldehydes ald.H$^+$, ald_2.H$^+$, intermediates int1, int1_2 in acetaldehyde and $i$-propyl aldehyde are shown in Figure 4.13. The HOMOs and LUMOs of intermediates int2, int2_2, int3, int3_2, transition states TS, TS_2 in acetaldehyde and $i$-propyl aldehyde. are shown in Figure 4.14. The HOMOs and LUMOs of α-hydroxy phosphonates ahp, ahp_2, in acetaldehyde and $i$-propyl aldehyde trimetylphosphite (tmp), methanal (MeOH), protonated-methanal (MeOH$_2^+$), water (H$_2$O) and hydronium ion (H$_3$O$^+$).are shown in Figure 4.15. All the HOMOs and LUMOs of species in acetaldehyde conversion system are very different from their corresponding orbitals of species in $i$-propyl aldehyde conversion system.

The B3LYP/6-311+G(d,p) HOMO, LUMO energies, interfrontier molecular orbital energy gaps, $\Delta E_{\text{HOMO-LUMO}}$ and chemical indices of all species in acetaldehyde and $i$-propyl aldehyde conversion systems are shown in Tables 4.8 and 4.9, respectively. These two tables show that the transition-state structures are the most reactive species as compared to their equivalent species in their conversion systems. Relative reactivities of the mass equivalent species for acetaldehyde and $i$-propyl aldehyde conversion systems are in decreasing orders: TS > int3 > ald.H$^+$ > int1 > int2 and TS_2 > int3_2 > ald_2.H$^+$> int2_2 > int1_2, respectively.
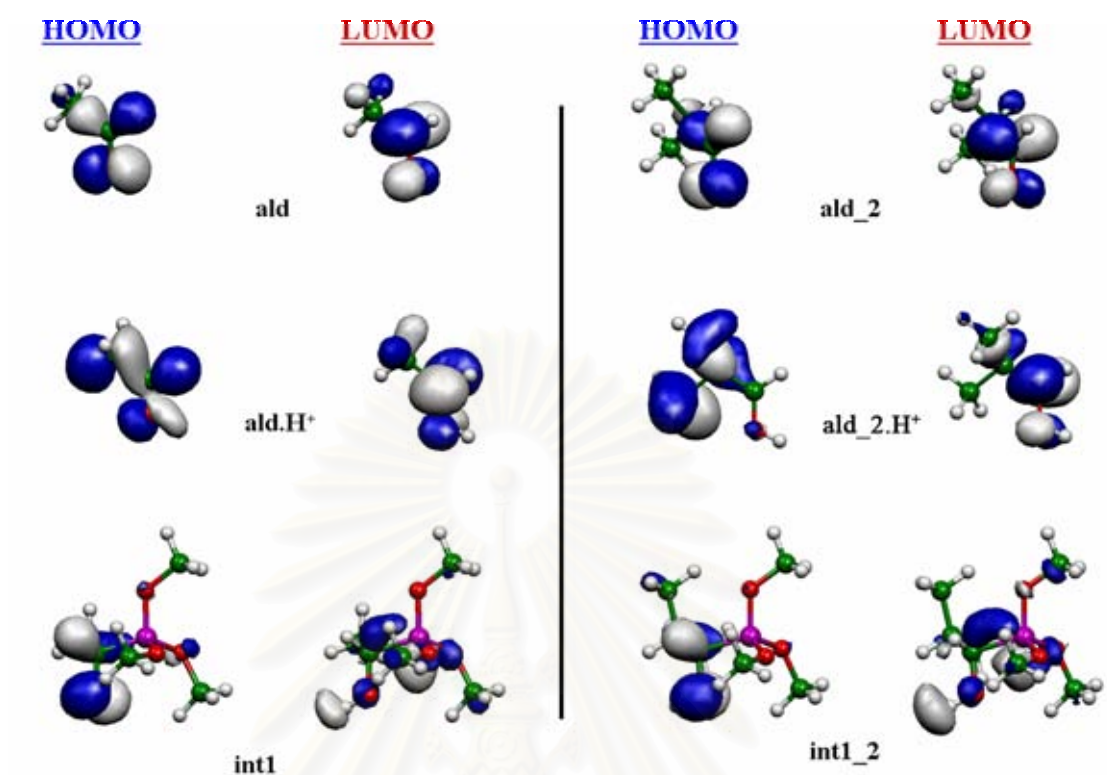
**Figure 4.13** The HOMOs and LUMOs of aldehydes ald, ald_2, protonated aldehydes ald.H⁺, ald_2.H⁺, intermediates int1, int1_2 in acetaldehyde (left) and *i*-propyl aldehyde (right).
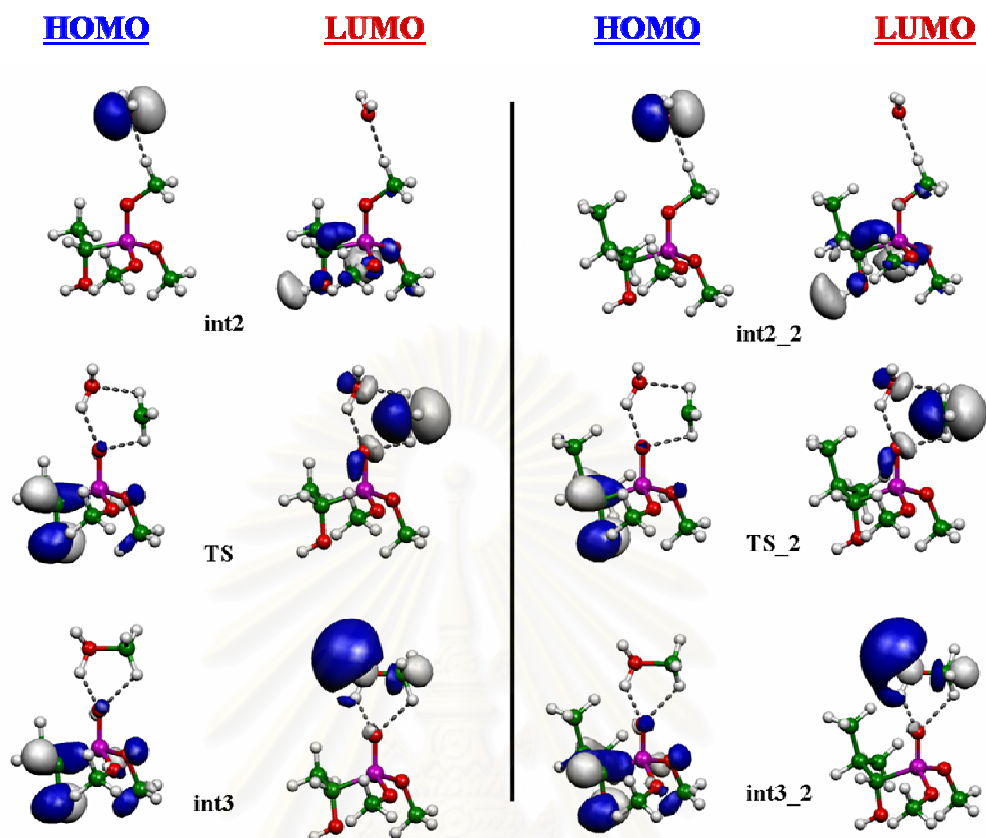
**Figure 4.14** The HOMOs and LUMOs of intermediates int2, int2_2, int3, int3_2, transition states TS, TS_2 in acetaldehyde (left) and *i*-propyl aldehyde (right).
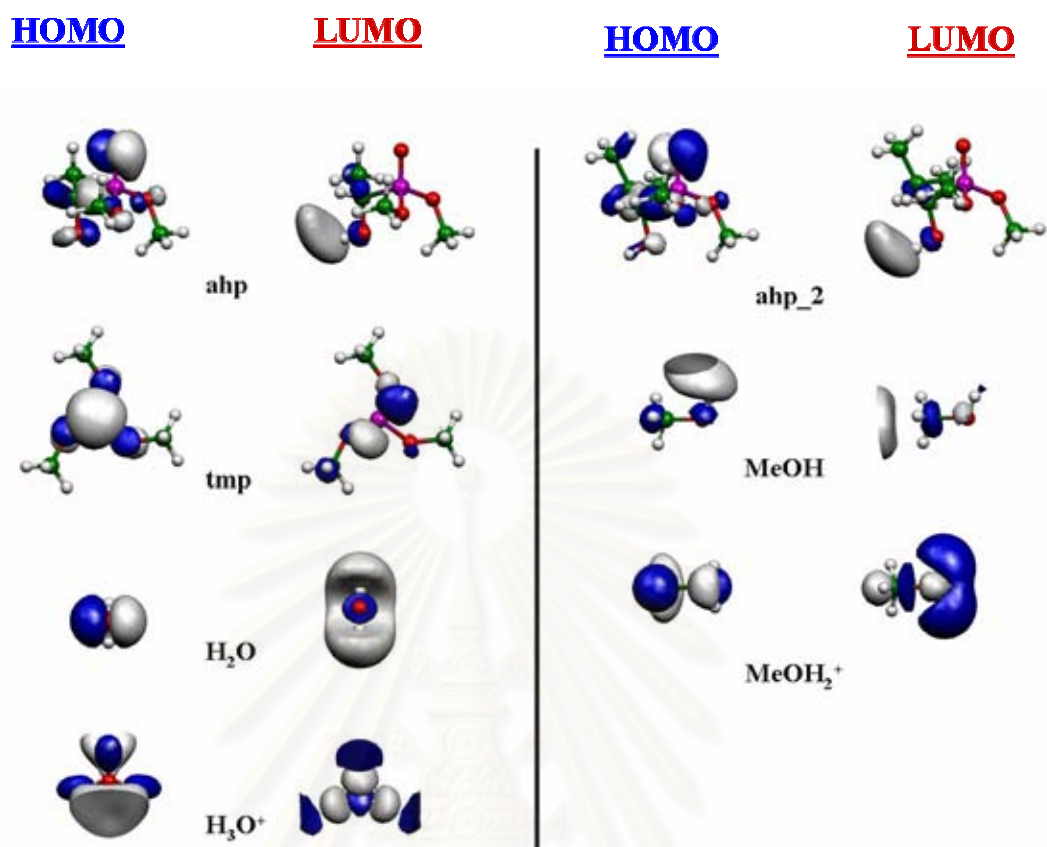
**Figure 4.15** The HOMOs and LUMOs of α-hydroxy phosphonates ahp, ahp_2, in acetaldehyde (left) and *i*-propyl aldehyde (right) trimetylphosphite (tmp), methanal (MeOH), protonated-methanal (MeOH$_2^+$), water (H$_2$O) and hydronium ion (H$_3$O$^+$).

**Table 4.8** The $E_{LUMO}$ and $E_{HOMO}$ energies and frontier molecular orbital energy gap, $\Delta E_{gap}$ of typical conformers derivatives computed at the B3LYP/6-311+G(d,p) level of theory in acetaldehyde system

| Conformer | $E_{LUMO (eV)}$[a] | $E_{HOMO (eV)}$[a] | $\Delta E_{gap}$[a,b] | $\eta$[a,c] | $\mu$[a,d] | $\chi$[a,e] |
|---|---|---|---|---|---|---|
| $H_2O$ | 0.52 | -8.79 | 9.31 | 4.65 | -4.13 | 4.13 |
| $H_3O^+$ | -7.58 | -20.29 | 12.71 | 6.35 | -13.93 | 13.93 |
| ald | -1.11 | -7.34 | 6.23 | 3.12 | -4.22 | 4.22 |
| ald.H$^+$ | -9.09 | -17.06 | 7.97 | 3.99 | -13.07 | 13.07 |
| int1 | -4.05 | -12.37 | 8.32 | 4.16 | -8.21 | 8.21 |
| int2 | -3.84 | -11.59 | 7.75 | 7.72 | -3.88 | 3.88 |
| int3 | -5.66 | -10.77 | 5.11 | 2.56 | -8.22 | 8.22 |
| TS | -7.90 | -11.67 | 3.77 | 1.88 | -9.79 | 9.79 |
| ahp | -0.41 | -7.80 | 7.39 | 3.70 | -4.11 | 4.11 |
| tmp | 0.08 | -6.64 | 6.72 | 3.36 | -3.28 | 3.28 |
| MeOH | -0.07 | -7.73 | 7.67 | 3.83 | -3.90 | 3.90 |
| MeOH$_2^+$ | -6.87 | -17.12 | 10.24 | 5.12 | -11.99 | 11.99 |

[a] In eV.

[b] $\Delta E_{gap} = \Delta E_{HOMO-LUMO}$

[c] Chemical hardness, $\eta = . \Delta E_{gap}/2$

[d] Electronic chemical potential, $\mu = (\Delta E_{HOMO} + \Delta E_{LUMO})/2$

[e] The mulliken electronegativity, $\chi = (\Delta E_{HOMO} - \Delta E_{LUMO})/2$.

**Table 4.9** The $E_{LUMO}$ and $E_{HOMO}$ energies and frontier molecular orbital energy gap, $\Delta E_{gap}$ of typical conformers derivatives computed at the B3LYP/6-311+G(d,p) level of theory in *i*-propyl aldehyde system

| Conformer | $E_{LUMO (eV)}$[a] | $E_{HOMO (eV)}$[a] | $\Delta E_{gap}$[a,b] | $\eta$[a,c] | $\mu$[a,d] | $\chi$[a,e] |
|---|---|---|---|---|---|---|
| $H_2O$ | 0.52 | -8.79 | 9.31 | 4.65 | -4.13 | 4.13 |
| $H_3O^+$ | -7.58 | -20.29 | 12.71 | 6.35 | -13.93 | 13.93 |
| ald_2 | -1.08 | -7.17 | 6.09 | 3.04 | -4.12 | 4.12 |
| ald_2.H$^+$ | -8.46 | -14.55 | 6.09 | 3.05 | -11.50 | 11.50 |
| int1_2 | -3.92 | -12.10 | 8.18 | 4.09 | -8.01 | 8.01 |
| int2_2 | -3.73 | -11.58 | 7.85 | 3.93 | -7.66 | 7.66 |
| int3_2 | -5.65 | -10.69 | 5.04 | 2.52 | -8.17 | 8.17 |
| TS_2 | -7.82 | -11.47 | 3.65 | 1.82 | -9.65 | 9.65 |
| ahp_2 | -0.44 | -7.71 | 7.27 | 3.63 | -4.07 | 4.07 |
| tmp | 0.08 | -6.64 | 6.72 | 3.36 | -3.28 | 3.28 |
| MeOH | -0.07 | -7.73 | 7.67 | 3.83 | -3.90 | 3.90 |
| $MeOH_2^+$ | -6.87 | -17.12 | 10.24 | 5.12 | -11.99 | 11.99 |

[a] In eV.

[b] $\Delta E_{gap} = \Delta E_{HOMO\text{-}LUMO}$

[c] Chemical hardness, $\eta = . \Delta E_{gap}/2$

[d] Electronic chemical potential, $\mu = (\Delta E_{HOMO} + \Delta E_{LUMO})/2$

[e] The mulliken electronegativity, $\chi = (\Delta E_{HOMO} - \Delta E_{LUMO})/2$.

# CHAPTER V

# CONCLUSION AND SUGGESTION

Conversion reaction of aldehyde as acetaldehyde to α-hydroxy phosphonate was computed at B3LYP/6-31G(d) and B3LYP/6-311G+(d,p) in gas phase. The results agree with the proposed mechanism in this work that obtained geometrical structure, energetics and thermodynamic quantities of intermediate2, transition state and intermediat3. The rate constants and thermodynamic quantities were resulted in very similar. These methods were confirmed accurately. Moreover, R group of aldehyde reactant was varied to *i*-propyl aldehyde for comparison the reaction step. The same results from both systems were observed. Furthermore, conversion reaction of aldehyde to α-hydroxy phosphonate of both systems were studied on rate constants in gas and aqueous phases by computational and CPCM model, respectively. The rate constants from these calculation methods revealed that acetaldehyde system gave the higher value than *i*-propyl aldehyde system in both gas and aqueous phases. From this results and energy profiles indicated that the synthesis of α-hydroxy phosphonate by hydrophosphonylation reaction using aldehye are exothermic reaction which aqueous phase is highly effective than gas phase in both systems. However, the reaction of acetaldehyde system is higher reactive than *i*-propyl aldehyde system in the same phase.

**Suggestion for further work**

Further studies will aim to extend the scope of this reaction and on further application of a variety reactant as aliphatic and aromatic aldehydes and provides the various of product.

# REFERENCES

1. Zhou, J.; Chen, R. Six-membered cyclic phosphate-phosphonates: Synthesis and stereochemistry of cistrans-2-phosphorylbenzyloxy-4-aryl-5,5-dimethl-1,3,2λ5-dioxaphosphorinane-2-thiones (selones). *J. Chem. Soc., Perkin trans*. 1 (1998): 2917.

2. Yamagishi, T.; Yokomatsu, T.; Suemune, K.; Shlbuya S. Enantioselective synthesis of α-hydroxyphosphinic acid derivatives through hydrophosphinylation of aldehydes catalyzed by AI-Li-BINOL complex. *Tetrahedron* 55 (1999): 12125-12136.

3. Blazis, V. J.; Koeller. K. J.; Spilling C. D. Application of Wallach's Rule in a comparison of the X-ray crystal structures of the racemate and the enantiomer of (1-Hydroxy-3-phenyl-2-propenyl)dimethyl-phosphonate *J. Org. Chem.* 60 (1995): 931.

4. Yokomatsu, T.; Yamagishi T.; Shibuya S. Enantioselective synthesis of á-hydroxyphosphonates through asymmetric Pudovik reactions with chiral lanthanoid and titanium alkoxides. *J. Chem. Soc., Perkin Trans.* 1 (1997): 1527-1533.

5. Yokomatsu, T.; Yamagishi, T.; Suemune, K.; Yoshida, Y.; Shibuya, S. Enantio-selective synthesis of threo-Dihydroxyphosphonates by asymmetric dihydroxylation of l-alkenylphosphonates with AD-mix reagents. *Tetrahedron* 54 (1998): 767-780.

6. Kozlowski, K. J.; Kath, P. N.; Spilling, D. C. Determination of the enantiomeric purity and absolute configuration of α-hydroxy phosphonates. *Tetrahedron* 51 (1995): 6385-6396.

7. Cao, X.; Mjalli, M. M. A. Combinatorial method for the synthesis of α–hydroxy phosphonates on Wang resin. *Tetrahedron Lett.* 37 (1996): 6073.

8. Sasai, H.; Bougauchi, M.; Arai, T.; Shibasaki, M. Enantioselective synthesis of α-hydroxy phosphonates using the LaLi3tris (binaphthoxide) catalyst (LLB), prepared by an improved method. *Tetrahedron Lett*. 38 (1997): 2717.

9.  Pogatchnik, M. D.; Wiemer, F. D. Enantioselective synthesis of α–hydroxy phosphonates *via* oxidation with (Camphorsulfonyl) oxaziridines. *Tetrahedron Lett.* 38 (1997): 3495.

10. Dolle, E. R.; Herpin, F. T.; Shimshock, C. Y. Solid-phase synthesis of α-hydroxy phosphonates and hydroxystatine amides. Transition-state isosteres derived from resin-bound amino acid aldehydes. *Tetrahedron Lett.* 42 (2001): 1855–1858.

11. Rowe J. B.; Spilling D. C. The synthesis of 1-hydroxy phosphonates of high enantiomeric excess using sequential asymmetric reactions: titanium alkoxide-catalyzed P-C bond formation and kinetic resolution. *Tetrahedron* 12 (2001): 1701–1708.

12. Boullet, T. F.; Foucaud, A. *Synthesis of dialkyl-hydroxymethylphosphonates in heterogeneous conditions*. Phosphorus, Sulfur, and Silicon and the Related Elements: Taylor & Francis, (2002).

13. Heydari, A.; Aref, I. A.; Khaksar, S.; Tajbakhsh, M. Hydrophosphonylation of aldehydes catalyzed by guanidine hydrochloride in water. *Catal. Commun.* 7 (2006): 982-984.

14. Jursic, B. S. Complete basis set and ab initio computational study of hydroniumi ion addition to ethylene as an example of acid interactions with unsaturated hydrocarbons. *J. Mol. Struct. (THEOCHEM)* 487 (1999): 163-175.

15. Jensen, F. *Introduction to computational chemistry*. Chichester: John Wiley & Sons, (1999).

16. Lewars, E. *Computational chemistry: Introduction to the theory and applications of molecular and quantum mechanics*. Trent University: Peter-borough, Ontario, (2003).

17. Koch, W.; Holthausen, C. M. *A Chemist's Guide to Density Functional Theory*. Chichester: John Wiley & Sons, (2000).

18. Barone, V.; Cossi, M. J.; Tomasi, C. J. Geometry optimization of molecular structures in solution by the polarizable continuum model. *J. Comput. Chem.* 19 (1998): 404.

19. Cossi, M.; Barone, V. Analytical second derivatives of the free energy in solution by polarizable continuum models. *J. Chem. Phys.* 109 (1988): 6246.

20. Takano, Y.; Houk, N. K. Benchmarking the Conductor-like Polarizable Continuum Model (CPCM) for aqueous solvation free energies of neutral and ionic organic molecules. *J. Chem. Theory Comput.* 1 (2005): 70-77.

21. Frisch, M. J.; Trucks, G. W.; Schlegel, H. B.; Scuseria, G. E.; Robb, M. A.; Cheeseman, J. R.; Montgomery, J. A.; Jr.; Vreven, T.; Kudin, K. N.; Burant, J. C.; Millam, J. M.; Iyengar, S. S.; Tomasi, J.; Barone, V.; Mennucci, B.; Cossi, M.; Scalmani, G.; Rega, N.; Petersson, G. A.; Nakatsuji, H.; Hada, M.; Ehara, M.; Toyota, K.; Fukuda, R.; Hasegawa, J.; Ishida, M.; Nakajima, T.; Honda, Y.; Kitao, O.; Nakai, H.; Klene, M.; Li, X.; Knox, J. E.; Hratchian, H. P.; Cross, J. B.; Adamo, C.; Jaramillo, J.; Gomperts, R.; Stratmann, R. E.; Yazyev, O.; Austin, A. J.; Cammi, R.; Pomelli, C.; Ochterski, J. W.; Ayala, P. Y.; Morokuma, K.; Voth, G. A.; Salvador, P.; Dannenberg, J. J.; Zakrzewski, V. G.; Dapprich, S.; Daniels, A. D.; Strain, M. C.; Farkas, O.; Malick, D. K.; Rabuck, A. D.; Raghavachari, K.; Foresman, J. B.; Ortiz, J. V.; Cui, Q.; Baboul, A. G.; Clifford, S.; Cioslowski, J.; Stefanov, B. B.; Liu, G.; Liashenko, A.; Piskorz, P.; Komaromi, I.; Martin, R. L.; Fox, D. J.; Keith, T.; Al-Laham, M. A.; Peng, C. Y.; Nanayakkara, A.; Challacombe, M.; Gill, P. M. W.; Johnson, B.; Chen, W.; Wong, M. W.; Gonzalez, C. and Pople, J. A. *Gaussian 03*. Revision B.03: Gaussian, Inc., Pittsburgh PA, (2003).

22. Caillet, J.; Claverie, P.; Pullman, B. On the conformational varieties of acetylcholine in the crystals of its halides. *Acta Cryst.* 34 (1978): 3266-3272.

23. Pope, M.; Swenberg, E. C. *Electronic Processes in Organic Crystals and Polymers.* 2nd ed. Oxford University Press: Oxford Science Publications (New York), (1999).

24. Anton, V. J.; Stanislav, Z. Modeling of charge-transfer transitions and excited states in $d^6$ transition metal complexes by DFT techniques coordination. *Chem. Rev.* 251 (2007): 258–287.

25. Domingo, R. L.; Saez, A. J.; Palmucci, C.; Arquesb, S. J.; Gonzalez-Rosendec, E. M. A DFT study for the formation of imidazo [1,2-c] pyrimidines through an intramolecular Michael addition. *Tetrahedron* 62 (2006): 10408–10416.

26. Becke, D. A. Density-Functional Thermochemistry .3. the Role of Exact exchange. *J. Chem. Phys.* 98 (1993): 5648.

27. Becke, D. Density-functional exchange-energy approximation with correcta-symptotic behavior. *Phys. Rev. A* 38 (1988): 3098.

28. Lee, C.; Yang, W.; Parr, R.G. Development of the Colle-Salvetti correlation energy formula into a functional of the electron density. *Phys. Rev. B* 37 (1988): 785.

29. Schaftenaar, G. *MOLDEN 4.2* CAOS/CAMM. Center Nijmegen: Toernooiveld, Nijmegen, Netherlands, (1991).

30. Flükiger, P.; Lüthi, P. H.; Portmann, S.; Weber, J. *MOLEKEL 4.3.* Swiss Center for Scientific Computing: Manno (Switzerland), (2000).

**APPENDICES**

# APPENDIX A



**Table A1** Geometry parameter of $H_2O$.
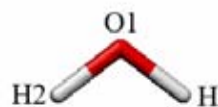
| Bond Length | Value (Angstroms) | Angle | Value (Degrees) |
|---|---|---|---|
| R(1,2) | 0.9620 | A(2,1,3) | 105.0609 |
| R(1,3) | 0.9620 | | |



**Table A2** Geometry parameter of $H_3O$.
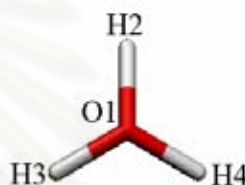
| Bond Length | Value (Angstroms) | Angle | Value (Degrees) |
|---|---|---|---|
| R(1,2) | 0.9799 | A(2,1,3) | 113.5380 |
| R(1,3) | 0.9799 | A(2,1,4) | 113.5380 |
| R(1,4) | 0.9799 | A(3,1,4) | 113.5379 |



**Table A3** Geometry parameter of $MeOH_2^+$.
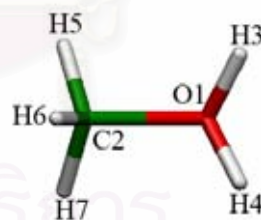
| Bond Length | Value (Angstroms) | Angle | Value (Degrees) | Dihedral | Value (Degrees) |
|---|---|---|---|---|---|
| R(1,2) | 1.5236 | A(2,1,3) | 115.4651 | A(5,2,1,3) | 55.6246 |
| R(1,3) | 0.9754 | A(2,1,4) | 115.4652 | A(6,2,1,3) | -65.6080 |
| R(1,4) | 0.9754 | A(3,1,4) | 110.6231 | A(1,2,1,3) | 173.1591 |
| R(2,5) | 1.0857 | A(5,2,1) | 104.3754 | A(5,2,1,4) | -173.1596 |
| R(2,6) | 1.0866 | A(6,2,1) | 108.0701 | A(6,2,1,4) | 65.6061 |
| R(2,7) | 1.0857 | A(7,2,1) | 104.3753 | A(1,2,1,4) | -65.6251 |
| | | A(5,2,6) | 113.6092 | | |
| | | A(6,2,7) | 113.6093 | | |
| | | A(5,2,7) | 111.8481 | | |
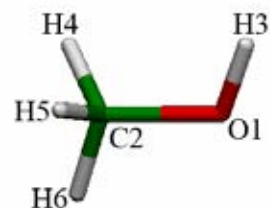
**Table A4** Geometry parameter of MeOH.

| Bond Length | Value (Angstroms) | Angle | Value (Degrees) | Dihedral | Value (Degrees) |
|---|---|---|---|---|---|
| R(1,2) | 1.4234 | A(2,1,3) | 108.8752 | A(4,2,1,3) | 61.4371 |
| R(1,3) | 0.9612 | A(4,2,1) | 112.1210 | A(5,2,1,3) | -61.5063 |
| R(2,4) | 1.0969 | A(5,2,1) | 112.1200 | A(6,2,1,3) | 179.5658 |
| R(2,5) | 1.0969 | A(6,2,1) | 106.7097 | | |
| R(2,6) | 1.0902 | A(4,2,5) | 108.9605 | | |
| | | A(5,2,6) | 108.3901 | | |
| | | A(4,2,6) | 108.3891 | | |
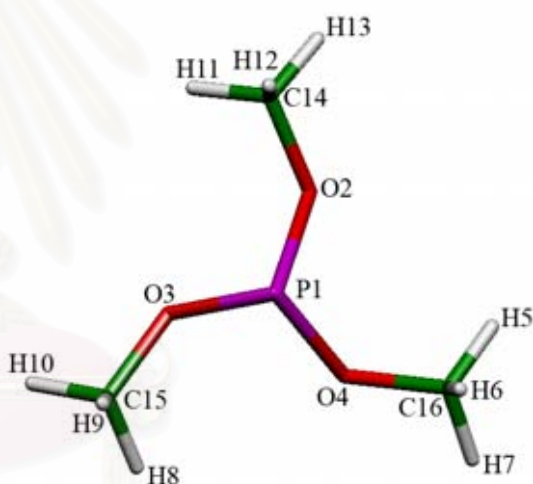


**Table A5** Geometry parameter of tmp.

| Bond Length | Value (Angstroms) | Angle | Value (Degrees) | Dihedral | Value (Degrees) |
|---|---|---|---|---|---|
| R(1,2) | 1.2656 | A(5,1,2) | 118.4616 | A(14,2,1,4) | -179.6129 |
| R(2,4) | 0.9778 | A(1,2,4) | 115.3470 | A(15,3,1,4) | 81.2288 |
| R(1,5) | 1.0938 | A(3,1,5) | 121.2997 | A(16,4,1,2) | 81.2288 |
| R(1,3) | 1.4475 | A(3,1,2) | 120.2386 | A(12,14,2,1) | 43.8660 |
| R(3,6) | 1.1018 | A(1,3,6) | 108.0365 | A(11,14,2,1) | -77.9807 |
| R(3,7) | 1.1018 | A(1,3,7) | 108.0452 | A(13,14,2,1) | 163.1092 |
| R(3,8) | 1.0882 | A(1,3,8) | 113.1691 | A(5,6,16,4) | -77.9808 |
| | | A(6,3,7) | 103.9966 | A(6,16,4,1) | 43.8661 |
| | | A(7,3,8) | 111.5510 | A(7,16,4,1) | 163.1092 |
| | | A(8,3,6) | 111.5545 | A(8,15,3,1) | -77.9807 |
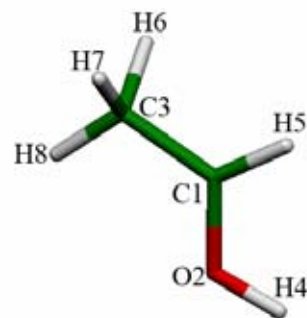
**Table A6** Geometry parameter of ald.H⁺.

| Bond Length | Value (Angstroms) | Angle | Value (Degrees) | Dihedral | Value (Degrees) |
|---|---|---|---|---|---|
| R(1,2) | 1.2656 | A(5,1,2) | 118.4616 | A(7,3,1,2) | 124.0167 |
| R(2,4) | 0.9778 | A(1,2,4) | 115.3470 | A(6,3,1,2) | -124.0448 |
| R(1,5) | 1.0938 | A(3,1,5) | 121.2997 | A(8,3,1,2) | -0.0085 |
| R(1,3) | 1.4475 | A(3,1,2) | 120.2386 | A(5,1,2,4) | 0.0093 |
| R(3,6) | 1.1018 | A(1,3,6) | 108.0365 | | |
| R(3,7) | 1.1018 | A(1,3,7) | 108.0452 | | |
| R(3,8) | 1.0882 | A(1,3,8) | 113.1691 | | |
| | | A(6,3,7) | 103.9966 | | |
| | | A(7,3,8) | 111.5510 | | |
| | | A(8,3,6) | 111.5545 | | |
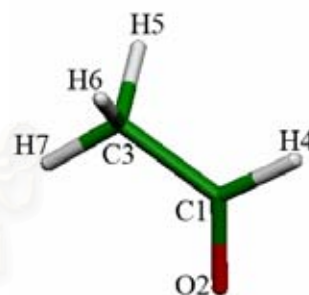
**Table A7** Geometry parameter of ald.

| Bond Length | Value (Angstroms) | Angle | Value (Degrees) | Dihedral | Value (Degrees) |
|---|---|---|---|---|---|
| R(1,2) | 1.2060 | A(4,1,2) | 120.0759 | A(6,3,1,2) | 121.7285 |
| R(1,4) | 1.1122 | A(4,1,3) | 115.0959 | A(7,3,1,2) | 0.0042 |
| R(1,3) | 1.5039 | A(1,3,5) | 109.4253 | A(5,3,1,2) | -121.7244 |
| R(3,5) | 1.0956 | A(1,3,6) | 109.4232 | A(5,3,1,4) | 58.2776 |
| R(3,6) | 1.0956 | A(1,3,7) | 110.9989 | A(6,3,1,4) | -58.2693 |
| R(3,7) | 1.0898 | A(5,3,6) | 106.6727 | A(7,3,1,4) | -179.9936 |
| | | A(6,3,7) | 110.1122 | | |
| | | A(7,3,5) | 110.1077 | | |
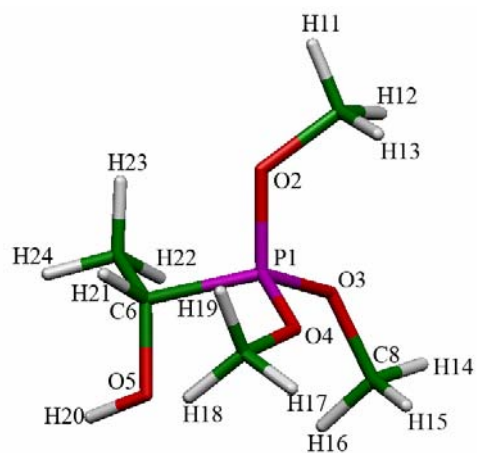
**Table A8** Geometry parameter of int1.

| Bond Length | Value (Angstroms) | Angle | Value (Degrees) | Dihedral | Value (Degrees) |
|---|---|---|---|---|---|
| R(1,2) | 1.5638 | A(2,1,3) | 107.4638 | A(2,1,6,5) | -172.3133 |
| R(1,3) | 1.5638 | A(2,1,4) | 113.6423 | A(6,1,3,8) | -83.6624 |
| R(1,4) | 1.5703 | A(3,1,4) | 105.4636 | A(2,1,3,8) | 161.6233 |
| R(1,6) | 1.8355 | A(4,1,6) | 112.4259 | A(1,6,5,20) | -170.4028 |
| R(2,10) | 1.4697 | A(2,1,6) | 104.0735 | | |
| R(3,8) | 1.4721 | A(3,1,6) | 113.8831 | | |
| R(4,7) | 1.4672 | A(1,3,8) | 127.2729 | | |
| R(6,5) | 1.4226 | A(1,2,10) | 126.6165 | | |
| R(6,9) | 1.5264 | A(1,4,7) | 127.7639 | | |
| R(10,11) | 1.0856 | A(1,6,5) | 102.1320 | | |
| R(10,12) | 1.0881 | A(1,6,9) | 112.4372 | | |
| R(10,13) | 1.0890 | A(5,6,9) | 114.5019 | | |
| R(8,14) | 1.0857 | A(2,10,11) | 104.9434 | | |
| R(8,15) | 1.0878 | A(2,10,12) | 109.0360 | | |
| R(8,16) | 1.0878 | A(2,10,13) | 109.5793 | | |
| R(7,17) | 1.0859 | A(11,10,12) | 110.9435 | | |
| R(7,18) | 1.0884 | A(11,10,13) | 110.7118 | | |
| R(7,19) | 1.0896 | A(12,10,13) | 111.4093 | | |
| R(5,20) | 0.9652 | A(3,8,14) | 104.7121 | | |
| R(6,21) | 1.0990 | A(3,8,15) | 109.1556 | | |
| R(9,22) | 1.0910 | A(3,8,16) | 109.1254 | | |
| R(9,23) | 1.0916 | A(14,8,15) | 111.0794 | | |
| R(9,24) | 1.0935 | A(14,8,16) | 111.1510 | | |
| | | A(15,8,16) | 111.3733 | | |
| | | A(4,7,17) | 104.9553 | | |
| | | A(4,7,18) | 108.9253 | | |
| | | A(4,7,19) | 109.9020 | | |
| | | A(17,7,19) | 110.2727 | | |
| | | A(17,7,18) | 110.6535 | | |
| | | A(19,7,18) | 111.8936 | | |
| | | A(6,5,20) | 109.8472 | | |
| | | A(1,6,21) | 106.1068 | | |
| | | A(5,6,21) | 111.2076 | | |
| | | A(21,6,9) | 109.9467 | | |
| | | A(6,9,22) | 111.5126 | | |
| | | A(6,9,23) | 111.0080 | | |
| | | A(6,9,24) | 108.8254 | | |
| | | A(24,9,23) | 107.5606 | | |
| | | A(24,9,22) | 108.6013 | | |
| | | A(23,9,22) | 109.2203 | | |
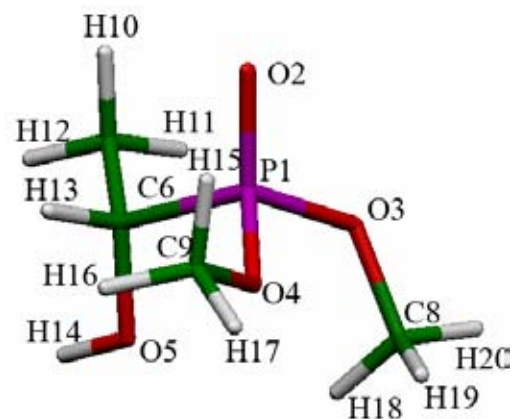
**Table A9** Geometry parameter of ahp.

| Bond Length | Value (Angstroms) | Angle | Value (Degrees) | Dihedral | Value (Degrees) |
|---|---|---|---|---|---|
| R(1,2) | 1.4797 | A(2,1,3) | 114.5354 | A(2,1,3,8) | 156.2117 |
| R(1,3) | 1.6002 | A(3,1,4) | 101.6740 | A(2,1,4,9) | 35.8312 |
| R(1,4) | 1.6186 | A(6,1,4) | 106.4289 | A(2,1,6,5) | 179.4100 |
| R(1,6) | 1.8482 | A(6,1,2) | 110.9923 | | |
| R(6,5) | 1.4307 | A(6,1,3) | 106.6227 | | |
| R(3,8) | 1.4449 | A(2,1,4) | 115.7036 | | |
| R(4,9) | 1.4390 | A(1,3,8) | 125.9218 | | |
| R(6,7) | 1.5274 | A(1,4,9) | 121.2406 | | |
| R(8,20) | 1.0886 | A(1,6,5) | 107.8188 | | |
| R(8,19) | 1.0901 | A(1,6,7) | 111.2901 | | |
| R(8,18) | 1.0897 | A(7,6,5) | 112.7508 | | |
| R(9,15) | 1.0911 | A(3,8,20) | 105.6558 | | |
| R(9,16) | 1.0934 | A(3,8,19) | 110.0456 | | |
| R(9,17) | 1.0888 | A(3,8,18) | 110.1917 | | |
| R(5,14) | 0.9633 | A(18,8,19) | 110.1627 | | |
| R(6,13) | 1.0993 | A(20,8,19) | 110.1537 | | |
| R(7,11) | 1.0920 | A(4,9,15) | 110.5844 | | |
| R(7,10) | 1.0915 | A(4,9,17) | 106.4170 | | |
| R(7,12) | 1.0954 | A(4,9,16) | 110.2919 | | |
| | | A(15,9,16) | 110.0781 | | |
| | | A(16,9,17) | 109.2988 | | |
| | | A(6,5,14) | 108.5454 | | |
| | | A(13,6,1) | 105.3250 | | |
| | | A(13,6,7) | 109.2856 | | |
| | | A(10,7,6) | 110.5170 | | |
| | | A(12,7,6) | 109.9376 | | |
| | | A(10,7,11) | 108.7309 | | |
| | | A(12,7,11) | 108.5533 | | |
| | | A(11,7,6) | 110.8320 | | |
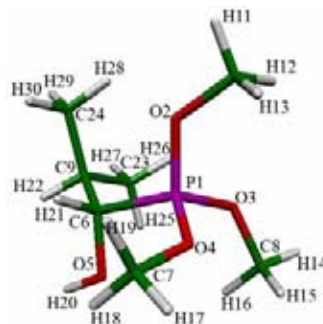
**Table A10** Geometry parameter of int1_2.

| Bond Length | Value (Angstroms) | Angle | Value (Degrees) | Dihedral | Value (Degrees) |
|---|---|---|---|---|---|
| R(1,2) | 1.5644 | A(2,1,3) | 107.2159 | A(2,1,3,8) | 162.5571 |
| R(1,3) | 1.5640 | A(2,1,4) | 112.8050 | A(2,1,4,7) | 79.8228 |
| R(1,4) | 1.5742 | A(3,1,4) | 104.7817 | A(2,1,6,5) | -175.6087 |
| R(1,6) | 1.8417 | A(4,1,6) | 110.8106 | A(2,1,6,9) | 59.5651 |
| R(2,10) | 1.4694 | A(2,1,6) | 105.6479 | A(1,6,9,23) | 56.9575 |
| R(3,8) | 1.4708 | A(3,1,6) | 115.7232 | A(1,6,9,24) | -73.0657 |
| R(4,7) | 1.4640 | A(1,3,8) | 126.9379 | A(24,9,6,5) | 169.1006 |
| R(6,5) | 1.4264 | A(1,2,10) | 125.9715 | | |
| R(6,9) | 1.5471 | A(1,4,7) | 127.8500 | | |
| R(10,11) | 1.0857 | A(1,6,5) | 100.2651 | | |
| R(10,12) | 1.0882 | A(1,6,9) | 118.7438 | | |
| R(10,13) | 1.0891 | A(5,6,9) | 114.0169 | | |
| R(8,14) | 1.0858 | A(2,10,11) | 104.9629 | | |
| R(8,15) | 1.0879 | A(2,10,12) | 109.1111 | | |
| R(8,16) | 1.0875 | A(2,10,13) | 109.6143 | | |
| R(7,17) | 1.0861 | A(11,10,12) | 110.9281 | | |
| R(7,18) | 1.0886 | A(11,10,13) | 110.6891 | | |
| R(7,19) | 1.0899 | A(12,10,13) | 111.3272 | | |
| R(5,20) | 0.9654 | A(3,8,14) | 104.7650 | | |
| R(6,21) | 1.1005 | A(3,8,15) | 109.0951 | | |
| R(9,22) | 1.1006 | A(3,8,16) | 109.1145 | | |
| R(9,23) | 1.5337 | A(14,8,15) | 111.0736 | | |
| R(9,24) | 1.5351 | A(14,8,16) | 111.1975 | | |
| R(23,25) | 1.0922 | A(15,8,16) | 111.3529 | | |
| R(23,26) | 1.0930 | A(4,7,17) | 105.0735 | | |
| R(23,27) | 1.0916 | A(4,7,18) | 108.9935 | | |
| R(24,28) | 1.0913 | A(4,7,19) | 110.0764 | | |
| R(24,29) | 1.0915 | A(17,7,19) | 110.1779 | | |
| R(24,30) | 1.0933 | A(17,7,18) | 110.5023 | | |
| | | A(19,7,18) | 111.7969 | | |
| | | A(6,5,20) | 109.5149 | | |
| | | A(1,6,21) | 104.4932 | | |
| | | A(5,6,21) | 110.7218 | | |
| | | A(21,6,9) | 108.0512 | | |
| | | A(6,9,23) | 114.4058 | | |
| | | A(6,9,24) | 112.7367 | | |
| | | A(9,23,25) | 112.1197 | | |
| | | A(9,23,26) | 111.7529 | | |
| | | A(9,23,27) | 109.4778 | | |
| | | A(27,23,26) | 107.3479 | | |
| | | A(27,23,25) | 107.4772 | | |
| | | A(25,23,26) | 108.4629 | | |
| | | A(9,24,28) | 111.9165 | | |
| | | A(9,24,29) | 109.3733 | | |
| | | A(9,24,30) | 111.9397 | | |
| | | A(30,24,29) | 107.5188 | | |
| | | A(30,24,28) | 108.2323 | | |
| | | A(29,24,28) | 107.6749 | | |
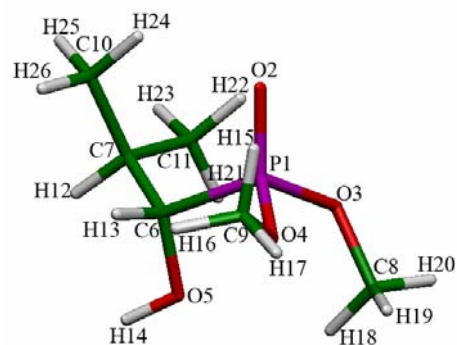
**Table A11** Geometry parameter of ahp_2.

| Bond Length | Value (Angstroms) | Angle | Value (Degrees) | Dihedral | Value (Degrees) |
|---|---|---|---|---|---|
| R(1,2) | 1.4807 | A(2,1,3) | 114.1304 | A(2,1,3,8) | 153.9138 |
| R(1,3) | 1.5985 | A(3,1,4) | 101.8711 | A(2,1,6,5) | 169.6651 |
| R(1,4) | 1.6221 | A(6,1,4) | 104.8256 | A(2,1,6,7) | 44.2886 |
| R(1,6) | 1.8552 | A(6,1,2) | 112.7019 | A(5,6,7,11) | -66.3662 |
| R(6,5) | 1.4324 | A(6,1,3) | 107.2538 | A(1,6,7,10) | -72.6826 |
| R(3,8) | 1.4440 | A(2,1,4) | 115.0201 | A(2,1,4,9) | 30.3986 |
| R(4,9) | 1.4391 | A(1,3,8) | 126.8000 | | |
| R(6,7) | 1.5458 | A(1,4,9) | 121.1933 | | |
| R(8,20) | 1.0888 | A(1,6,5) | 105.7577 | | |
| R(8,19) | 1.0900 | A(1,6,7) | 116.3145 | | |
| R(8,18) | 1.0892 | A(7,6,5) | 112.2756 | | |
| R(9,15) | 1.0909 | A(3,8,20) | 105.7212 | | |
| R(9,16) | 1.0937 | A(3,8,19) | 110.2178 | | |
| R(9,17) | 1.0890 | A(3,8,18) | 109.8693 | | |
| R(5,14) | 0.9633 | A(18,8,19) | 110.1909 | | |
| R(6,13) | 1.1001 | A(20,8,19) | 110.1443 | | |
| R(7,11) | 1.5342 | A(4,9,15) | 110.6450 | | |
| R(7,10) | 1.5353 | A(4,9,17) | 106.4567 | | |
| R(7,12) | 1.1016 | A(4,9,16) | 110.2990 | | |
| R(11,21) | 1.0920 | A(15,9,16) | 109.9052 | | |
| R(11,22) | 1.0929 | A(16,9,17) | 109.3066 | | |
| R(11,23) | 1.0934 | A(6,5,14) | 108.5244 | | |
| R(10,24) | 1.0911 | A(13,6,1) | 104.4450 | | |
| R(10,25) | 1.0934 | A(13,6,7) | 107.8917 | | |
| R(10,26) | 1.0949 | A(10,7,6) | 112.2290 | | |
| | | A(12,7,6) | 103.7563 | | |
| | | A(10,7,11) | 112.0411 | | |
| | | A(12,7,11) | 107.4122 | | |
| | | A(11,7,6) | 113.5248 | | |
| | | A(7,11,21) | 111.4050 | | |
| | | A(7,11,22) | 111.2091 | | |
| | | A(7,11,23) | 110.0159 | | |
| | | A(21,11,22) | 108.1756 | | |
| | | A(21,11,23) | 108.1395 | | |
| | | A(22,11,23) | 107.7671 | | |
| | | A(7,10,24) | 111.1340 | | |
| | | A(7,10,25) | 109.9369 | | |
| | | A(7,10,26) | 111.3963 | | |
| | | A(24,10,25) | 108.6196 | | |
| | | A(24,10,26) | 108.0093 | | |
| | | A(25,10,26) | 107.6286 | | |
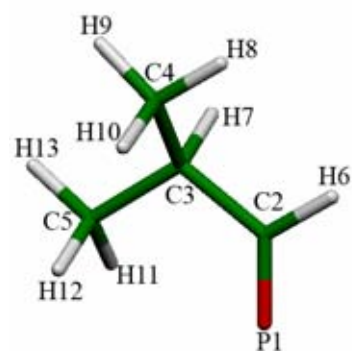
**Table A12** Geometry parameter of ald_2.

| Bond Length | Value (Angstroms) | Angle | Value (Degrees) | Dihedral | Value (Degrees) |
|---|---|---|---|---|---|
| R(1,2) | 1.2059 | A(1,2,6) | 120.1202 | A(4,3,2,1) | 126.4275 |
| R(2,6) | 1.1138 | A(1,2,3) | 125.5695 | A(5,3,2,1) | -0.1521 |
| R(2,3) | 1.5158 | A(3,2,6) | 114.3099 | A(7,3,2,1) | -119.0637 |
| R(3,4) | 1.5412 | A(2,3,5) | 112.6988 | A(5,3,2,6) | -179.9450 |
| R(3,5) | 1.5279 | A(2,3,4) | 109.2831 | | |
| R(3,7) | 1.1014 | A(2,3,7) | 104.6484 | | |
| R(4,8) | 1.0939 | A(4,3,5) | 113.0484 | | |
| R(4,9) | 1.0938 | A(3,5,11) | 110.8371 | | |
| R(4,10) | 1.0923 | A(3,5,12) | 111.2911 | | |
| R(5,11) | 1.0930 | A(3,5,13) | 110.4545 | | |
| R(5,12) | 1.0915 | A(11,5,12) | 107.3784 | | |
| R(5,13) | 1.0930 | A(11,5,13) | 108.2408 | | |
| | | A(12,5,13) | 108.5208 | | |
| | | A(3,4,8) | 110.8045 | | |
| | | A(3,4,9) | 111.7528 | | |
| | | A(3,4,10) | 110.3422 | | |
| | | A(8,4,9) | 108.0786 | | |
| | | A(8,4,10) | 107.9338 | | |
| | | A(10,4,9) | 107.7889 | | |

**Table A13** Geometry parameter of ald_2.H⁺.

| Bond Length | Value (Angstroms) | Angle | Value (Degrees) | Dihedral | Value (Degrees) |
|---|---|---|---|---|---|
| R(1,2) | 1.2059 | A(1,2,6) | 120.1202 | A(4,3,2,1) | 115.9161 |
| R(2,6) | 1.1138 | A(1,2,3) | 125.5695 | A(5,3,2,1) | -10.4952 |
| R(2,3) | 1.5158 | A(3,2,6) | 114.3099 | A(7,3,2,1) | -34.0973 |
| R(3,4) | 1.5412 | A(2,3,5) | 112.6988 | A(6,2,1,14) | 0.2130 |
| R(3,5) | 1.5279 | A(2,3,4) | 109.2831 | | |
| R(3,7) | 1.1014 | A(2,3,7) | 104.6484 | | |
| R(4,8) | 1.0939 | A(4,3,5) | 113.0484 | | |
| R(4,9) | 1.0938 | A(3,5,11) | 110.8371 | | |
| R(4,10) | 1.0923 | A(3,5,12) | 111.2911 | | |
| R(5,11) | 1.0930 | A(3,5,13) | 110.4545 | | |
| R(5,12) | 1.0915 | A(11,5,12) | 107.3784 | | |
| R(5,13) | 1.0930 | A(11,5,13) | 108.2408 | | |
| R(1,14) | 0.9762 | A(12,5,13) | 108.5208 | | |
| | | A(3,4,8) | 110.8045 | | |
| | | A(3,4,9) | 111.7528 | | |
| | | A(3,4,10) | 110.3422 | | |
| | | A(8,4,9) | 108.0786 | | |
| | | A(8,4,10) | 107.9338 | | |
| | | A(10,4,9) | 107.7889 | | |
| | | A(2,1,14) | 114.9211 | | |

# APPENDIX B

**Table B1** Cartesian coordinates of $H_2O$.

| Atomic Type | Coordinate (Angstroms) | | |
|:-----------:|:----------:|:----------:|:----------:|
| | X | Y | Z |
| O | 0.00000000 | 0.11705400 | 0.00000000 |
| H | 0.76357600 | -0.46821400 | 0.00000000 |
| H | -0.76357600 | -0.46821400 | 0.00000000 |

**Table B2** Cartesian coordinates of $H_3O$.

| Atomic Type | Coordinate (Angstroms) | | |
|:-----------:|:----------:|:----------:|:----------:|
| | X | Y | Z |
| O | 0.00000000 | 0.00000000 | 0.06922700 |
| H | 0.00000000 | 0.94649800 | -0.18460500 |
| H | 0.81969100 | -0.47324900 | -0.18460500 |
| H | -0.81969100 | -0.47324900 | -0.18460500 |

**Table B3** Cartesian coordinates of $MeOH_2^+$.

| Atomic Type | Coordinate (Angstroms) | | |
|:-----------:|:----------:|:----------:|:----------:|
| | X | Y | Z |
| H | 1.16236800 | -0.80207900 | 0.25183800 |
| O | 0.71973500 | 0.00000000 | -0.08322100 |
| H | 1.16236700 | 0.80208000 | 0.25183600 |
| C | -0.80050300 | 0.00000000 | 0.01793500 |
| H | -1.06823700 | -0.00000200 | 1.07112100 |
| H | -1.10568100 | 0.89932700 | -0.50831500 |
| H | -1.10568000 | -0.89932400 | -0.50832100 |

**Table B4** Cartesian coordinates of MeOH.

| Atomic Type | Coordinate (Angstroms) | | |
|---|---|---|---|
| | X | Y | Z |
| O | -0.74931200 | 0.12198300 | 0.00000100 |
| H | -1.14965900 | -0.75189200 | 0.00001200 |
| C | 0.66698900 | -0.02034800 | 0.00000200 |
| H | 1.08328500 | 0.98724500 | -0.00063400 |
| H | 1.02951400 | -0.54402600 | 0.89316100 |
| H | 1.02942400 | -0.54510500 | -0.89255800 |

**Table B5** Cartesian coordinates of tmp.

| Atomic Type | Coordinate (Angstroms) | | |
|---|---|---|---|
| | X | Y | Z |
| P | 0.00000000 | 0.00000000 | 0.46741700 |
| O | 0.90328500 | -1.11736600 | -0.34397700 |
| O | 0.51602500 | 1.34095100 | -0.34397700 |
| O | -1.41931000 | -0.22358400 | -0.34397700 |
| C | 0.00000000 | 2.62655500 | 0.01849000 |
| H | 0.67296500 | 3.36966600 | -0.40819200 |
| H | -1.00254300 | 2.76470900 | -0.39448300 |
| H | -0.03374800 | 2.75475400 | 1.10647100 |
| C | 2.27466300 | -1.31327700 | 0.01849000 |
| H | 2.58173400 | -2.26763800 | -0.40819200 |
| H | 2.89558000 | -0.51412700 | -0.39448300 |
| H | 2.40256100 | -1.34815100 | 1.10647100 |
| C | -2.27466300 | -1.31327700 | 0.01849000 |
| H | -3.25469900 | -1.10202800 | -0.40819200 |
| H | -1.89303700 | -2.25058300 | -0.39448300 |
| H | -2.36881300 | -1.40660300 | 1.10647100 |

**Table B6**  Cartesian coordinates of ald.

| Atomic Type | Coordinate (Angstroms) | | |
|---|---|---|---|
| | X | Y | Z |
| C | -0.23350800 | 0.39671000 | 0.00000100 |
| H | -0.30820700 | 1.50643800 | -0.00003900 |
| O | -1.23419000 | -0.27640300 | 0.00000100 |
| C | 1.16827200 | -0.14827100 | 0.00000500 |
| H | 1.16359200 | -1.23812600 | -0.00006700 |
| H | 1.70480600 | 0.22615800 | -0.87885600 |
| H | 1.70474500 | 0.22612200 | 0.87891200 |

**Table B7**  Cartesian coordinates of ald_2.

| Atomic Type | Coordinate (Angstroms) | | |
|---|---|---|---|
| | X | Y | Z |
| C | -0.93840900 | -0.61589500 | -0.20154600 |
| H | -1.00848300 | -1.68001900 | -0.52294600 |
| O | -1.89952700 | -0.06209600 | 0.27165900 |
| C | 0.42541600 | 0.01120800 | -0.41258700 |
| H | 0.59105900 | -0.04175600 | -1.50021700 |
| C | 0.48069300 | 1.46910000 | 0.04155400 |
| C | 1.49951300 | -0.86983600 | 0.25483200 |
| H | -0.29012500 | 2.06649700 | -0.44883100 |
| H | 1.45642400 | 1.90430400 | -0.18915000 |
| H | 0.31757600 | 1.54698800 | 1.11953900 |
| H | 1.39330200 | -0.85431200 | 1.34350800 |
| H | 2.49844300 | -0.50246700 | 0.00906400 |
| H | 1.43474000 | -1.90992600 | -0.07776100 |

**Table B8** Cartesian coordinates of ald.H$^+$.

| Atomic Type | Coordinate (Angstroms) | | |
| --- | --- | --- | --- |
| | X | Y | Z |
| C | 0.10951700 | 0.42780500 | 0.00006000 |
| H | 0.24749300 | 1.51293900 | -0.00013800 |
| O | 1.13719500 | -0.31087300 | -0.00000200 |
| C | -1.21230300 | -0.16218400 | -0.00002900 |
| H | -1.76274700 | 0.23389500 | 0.86841500 |
| H | -1.76301500 | 0.23437700 | -0.86806500 |
| H | -1.19550800 | -1.25034500 | -0.00029800 |
| H | 1.99293500 | 0.16239800 | -0.00008400 |

**Table B9** Cartesian coordinates of ald _2.H$^+$.

| Atomic Type | Coordinate (Angstroms) | | |
| --- | --- | --- | --- |
| | X | Y | Z |
| C | 0.84760600 | -0.54682200 | 0.33503300 |
| H | 1.06813600 | -1.52125500 | 0.77969000 |
| O | 1.77348200 | 0.04267100 | -0.30637100 |
| H | 2.61928600 | -0.44315300 | -0.34728600 |
| C | -0.47940900 | 0.02875300 | 0.43694000 |
| H | -0.74661200 | -0.07386700 | 1.50226400 |
| C | -0.61821500 | 1.47067600 | -0.04722000 |
| C | -1.43272700 | -0.98487600 | -0.31265900 |
| H | 0.05315400 | 2.14257600 | 0.49042200 |
| H | -1.64119100 | 1.80680700 | 0.12369800 |
| H | -0.40920600 | 1.55527800 | -1.11553700 |
| H | -1.22914700 | -0.98143800 | -1.38397000 |
| H | -2.45010100 | -0.63039200 | -0.14489400 |
| H | -1.35570700 | -2.00230400 | 0.07402800 |

**Table B10**  Cartesian coordinates of int1.

| Atomic Type | Coordinate (Angstroms) | | |
|:---:|:---:|:---:|:---:|
| | X | Y | Z |
| C | -1.37148100 | -0.37584200 | -0.83580500 |
| H | -1.25514200 | -0.08194200 | -1.88837300 |
| C | -1.76354600 | -1.84833300 | -0.74659000 |
| H | -1.03786400 | -2.47856800 | -1.26405500 |
| H | -1.85020200 | -2.17720700 | 0.29014500 |
| H | -2.73043600 | -1.98646100 | -1.23832200 |
| O | -2.24619600 | 0.51037600 | -0.14767500 |
| H | -3.16187400 | 0.31453800 | -0.38189600 |
| P | 0.24077200 | -0.03002200 | -0.02933600 |
| O | 0.33941800 | -0.55597000 | 1.44005300 |
| O | 0.55124000 | 1.50702100 | 0.05439600 |
| O | 1.27421000 | -0.83284500 | -0.88554400 |
| C | -0.13853000 | 0.11390400 | 2.66075900 |
| H | 0.20704600 | -0.51642500 | 3.47451700 |
| H | 0.30331500 | 1.10620700 | 2.71970800 |
| H | -1.22499000 | 0.16441800 | 2.63750900 |
| C | 0.27199000 | 2.53635200 | -0.95328100 |
| H | 0.68479700 | 3.45203300 | -0.54040000 |
| H | 0.77153400 | 2.28507300 | -1.88850800 |
| H | -0.80555700 | 2.62371900 | -1.07944900 |
| C | 2.68678000 | -1.07199400 | -0.55750600 |
| H | 2.74452200 | -1.65012200 | 0.36258800 |
| H | 3.07708800 | -1.63886300 | -1.39715200 |
| H | 3.20552800 | -0.11924800 | -0.46157400 |

**Table B11**  Cartesian coordinates of int1_2.

| Atomic Type | Coordinate (Angstroms) | | |
|---|---|---|---|
| | X | Y | Z |
| C | 0.86829500 | -0.52615300 | -0.88795700 |
| H | 0.72123000 | -0.16589900 | -1.91739200 |
| O | 0.61708200 | -1.92768100 | -0.80298100 |
| H | 1.35491700 | -2.41191100 | -1.19446900 |
| P | -0.58363300 | 0.12438800 | 0.03989200 |
| O | -0.62862700 | -0.22694600 | 1.56334500 |
| O | -1.92600100 | -0.45338800 | -0.54536600 |
| O | -0.49349000 | 1.68215000 | -0.07359900 |
| C | -1.06350700 | -1.49664600 | 2.16518500 |
| H | -1.01693100 | -1.32541300 | 3.23638900 |
| H | -2.08158100 | -1.71095100 | 1.84720500 |
| H | -0.37973200 | -2.28657500 | 1.86312300 |
| C | -2.26269900 | -0.69677000 | -1.94923200 |
| H | -3.30162000 | -1.01352200 | -1.93972600 |
| H | -2.15522700 | 0.22267200 | -2.52459300 |
| H | -1.62537800 | -1.49116100 | -2.33387200 |
| C | -1.36879600 | 2.64899100 | 0.60343200 |
| H | -1.24224400 | 2.55130200 | 1.67985600 |
| H | -1.03057100 | 3.62184300 | 0.25987400 |
| H | -2.40273900 | 2.47495200 | 0.30874700 |
| C | 2.28807700 | -0.11218900 | -0.43339100 |
| H | 2.92626700 | -0.74407800 | -1.06961700 |
| C | 2.62141100 | 1.34517300 | -0.78221100 |
| H | 2.40822400 | 1.57346200 | -1.82999600 |
| H | 2.06757000 | 2.04993400 | -0.15968300 |
| H | 3.68570300 | 1.52264400 | -0.61722900 |
| C | 2.60963100 | -0.45067800 | 1.02761100 |
| H | 2.07469900 | 0.20240600 | 1.72192100 |
| H | 2.36827100 | -1.48743000 | 1.27229900 |
| H | 3.67745600 | -0.31152700 | 1.20698000 |

**Table B12** Cartesian coordinates of int2.

| Atomic Type | Coordinate (Angstroms) | | |
|---|---|---|---|
| | X | Y | Z |
| C | 1.10031500 | 1.34973400 | -0.67946700 |
| H | 0.61416500 | 1.47070200 | -1.65757900 |
| C | 0.87246200 | 2.59604300 | 0.17203400 |
| H | -0.19306400 | 2.81037500 | 0.27321000 |
| H | 1.31303000 | 2.48734700 | 1.16440900 |
| H | 1.33694600 | 3.45286900 | -0.32395000 |
| O | 2.46666400 | 0.98030600 | -0.82724200 |
| H | 2.98736100 | 1.75144000 | -1.08331600 |
| O | -5.13920800 | 0.41261900 | -0.19637300 |
| H | -5.80775900 | -0.10487700 | -0.65799100 |
| H | -5.60424100 | 1.19341000 | 0.12282600 |
| P | 0.36653700 | -0.15503700 | 0.07230300 |
| O | 0.83214100 | -0.40821400 | 1.54411700 |
| O | 0.75502800 | -1.46067000 | -0.71475200 |
| O | -1.16500300 | 0.13368700 | 0.09213000 |
| C | 2.06355700 | -1.07973200 | 1.98625600 |
| H | 1.97497600 | -1.13584800 | 3.06705200 |
| H | 2.10639800 | -2.07350400 | 1.54577600 |
| H | 2.92309200 | -0.48032800 | 1.69371300 |
| C | 0.79577700 | -1.63194200 | -2.16904200 |
| H | 0.99345100 | -2.68859800 | -2.32396900 |
| H | -0.16626100 | -1.36080700 | -2.60361400 |
| H | 1.60633200 | -1.02836300 | -2.57397000 |
| C | -2.20584400 | -0.67943600 | 0.75579800 |
| H | -2.07929200 | -0.58343300 | 1.83234600 |
| H | -2.10617400 | -1.71707200 | 0.43916500 |
| H | -3.15159600 | -0.25759400 | 0.42482900 |

**Table B13** Cartesian coordinates of int2_2.

| Atomic Type | Coordinate (Angstroms) | | |
|---|---|---|---|
| | X | Y | Z |
| C | 1.04439100 | 0.81458400 | -0.90636100 |
| H | 0.62535200 | 0.70429500 | -1.91790100 |
| O | 2.42434800 | 0.45162600 | -0.88980200 |
| H | 2.94220400 | 1.13504200 | -1.33316000 |
| P | 0.32619500 | -0.58270400 | 0.05366600 |
| O | 0.82727500 | -0.70049500 | 1.53078800 |
| O | 0.70595100 | -1.96386700 | -0.60587800 |
| O | -1.21205600 | -0.32887100 | 0.09312300 |
| C | 2.09626400 | -1.27638200 | 1.99610300 |
| H | 2.02165800 | -1.27278400 | 3.07944600 |
| H | 2.19002500 | -2.29110700 | 1.61496900 |
| H | 2.91724200 | -0.64910900 | 1.65639300 |
| C | 0.73602500 | -2.28671900 | -2.03098300 |
| H | 0.91168600 | -3.35776500 | -2.07675800 |
| H | -0.22104000 | -2.04360300 | -2.49286300 |
| H | 1.55743000 | -1.74773400 | -2.50076900 |
| C | -2.20620300 | -1.13608100 | 0.83022200 |
| H | -2.01390700 | -1.03071700 | 1.89631200 |
| H | -3.17107900 | -0.71633300 | 0.55645600 |
| H | -2.12409400 | -2.17662700 | 0.51782600 |
| C | 0.76769300 | 2.25920700 | -0.42696400 |
| H | 1.43737000 | 2.84957700 | -1.07068600 |
| C | -0.66406300 | 2.71878700 | -0.73647300 |
| H | -0.92799500 | 2.55050200 | -1.78432100 |
| H | -1.40009000 | 2.20603100 | -0.11542300 |
| H | -0.75111500 | 3.78977100 | -0.54376700 |
| C | 1.16801700 | 2.52750300 | 1.02874200 |
| H | 0.48301900 | 2.04579700 | 1.73131600 |
| H | 2.18177700 | 2.18299700 | 1.24378600 |
| H | 1.13550000 | 3.60082000 | 1.22563200 |
| O | -5.11673500 | 0.13008200 | 0.00572300 |
| H | -5.58888500 | 0.85137700 | 0.43597800 |
| H | -5.78098000 | -0.32305800 | -0.52481700 |

**Table B14** Cartesian coordinates of TS.

| Atomic Type | Coordinate (Angstroms) | | |
|---|---|---|---|
| | X | Y | Z |
| C | 1.08058900 | 1.33980400 | -0.49079700 |
| H | 0.90204800 | 1.49792700 | -1.56420600 |
| C | 0.56317500 | 2.54204000 | 0.29699600 |
| H | -0.49392400 | 2.72298700 | 0.09153900 |
| H | 0.69852800 | 2.39994900 | 1.37050200 |
| H | 1.11509400 | 3.43632800 | -0.00584500 |
| O | 2.45063900 | 1.04028400 | -0.24417000 |
| H | 2.98440600 | 1.83188300 | -0.38437400 |
| O | -3.66842100 | 0.70203100 | -0.69360300 |
| H | -2.77647300 | 0.70392800 | -1.08205500 |
| H | -4.28292800 | 0.37647600 | -1.36451000 |
| P | 0.18093100 | -0.21157700 | -0.05794200 |
| O | 0.26833700 | -0.49982700 | 1.50156800 |
| O | 0.92949600 | -1.45093900 | -0.70195800 |
| O | -1.28947400 | -0.08337800 | -0.42045100 |
| C | 1.45223300 | -1.00379700 | 2.20251800 |
| H | 1.16444700 | -1.05349800 | 3.24917100 |
| H | 1.70014200 | -1.99299800 | 1.82212000 |
| H | 2.28360200 | -0.31618500 | 2.06079400 |
| C | 1.38969600 | -1.55637500 | -2.07835900 |
| H | 1.75892200 | -2.57287600 | -2.18406300 |
| H | 0.56157600 | -1.38972800 | -2.76838800 |
| H | 2.19812000 | -0.84536100 | -2.24617900 |
| C | -2.98481800 | -0.77732700 | 0.94351000 |
| H | -2.09692600 | -0.69325400 | 1.55141900 |
| H | -3.10341400 | -1.65030500 | 0.31802000 |
| H | -3.85703700 | -0.21305700 | 1.23088600 |

**Table B15**  Cartesian coordinates of TS_2.

| Atomic Type | Coordinate (Angstroms) | | |
|---|---|---|---|
| | X | Y | Z |
| C | 1.19062500 | 0.66636500 | -0.79080100 |
| H | 0.95914300 | 0.63017400 | -1.86669800 |
| C | 1.04034600 | 2.13616000 | -0.32827400 |
| H | 1.85832500 | 2.64087900 | -0.86411000 |
| O | 2.48957900 | 0.12903100 | -0.54627900 |
| H | 3.15635000 | 0.73329900 | -0.89577000 |
| O | -3.70981900 | 0.67911300 | -0.50651300 |
| H | -2.84894000 | 0.59524100 | -0.95201800 |
| H | -4.39136300 | 0.37392100 | -1.11992000 |
| P | 0.06655100 | -0.60691200 | -0.05058200 |
| O | 0.24383800 | -0.74626400 | 1.52177600 |
| O | 0.53211800 | -2.03208600 | -0.57609700 |
| O | -1.39361800 | -0.27994200 | -0.31729200 |
| C | 1.38401000 | -1.37485400 | 2.19174100 |
| H | 1.21378300 | -1.21796100 | 3.25353400 |
| H | 1.39618100 | -2.43705800 | 1.95424000 |
| H | 2.30831400 | -0.89826200 | 1.87303000 |
| C | 0.83703500 | -2.38997500 | -1.95035300 |
| H | 1.00088800 | -3.46439600 | -1.94261000 |
| H | -0.00345900 | -2.14974500 | -2.60322700 |
| H | 1.74538300 | -1.87781000 | -2.26688400 |
| C | -3.06046300 | -0.75607700 | 1.16906400 |
| H | -2.13605700 | -0.70647400 | 1.72392400 |
| H | -3.28082400 | -1.65324500 | 0.60918200 |
| H | -3.87091700 | -0.11300200 | 1.47087700 |
| C | -0.26477000 | 2.78301700 | -0.81164800 |
| H | -0.42805800 | 2.62096200 | -1.88117300 |
| H | -1.13093800 | 2.40049500 | -0.26806400 |
| H | -0.22373100 | 3.86153700 | -0.64694600 |
| C | 1.27185800 | 2.35292200 | 1.17230400 |
| H | 0.45662700 | 1.93664100 | 1.76933400 |
| H | 2.20760600 | 1.90189200 | 1.50849400 |
| H | 1.32480100 | 3.42242400 | 1.38657500 |

**Table B16** Cartesian coordinates of int3.

| Atomic Type | Coordinate (Angstroms) | | |
|---|---|---|---|
| | X | Y | Z |
| C | 1.16407200 | 1.12858700 | -0.80593300 |
| H | 0.84154000 | 1.05915200 | -1.85525600 |
| C | 0.86216100 | 2.52689000 | -0.27459900 |
| H | -0.19712700 | 2.77122800 | -0.37690700 |
| H | 1.14735600 | 2.62170000 | 0.77351000 |
| H | 1.42520600 | 3.26229200 | -0.85561600 |
| O | 2.53326300 | 0.75994500 | -0.68331000 |
| H | 3.08598400 | 1.44381500 | -1.07787100 |
| O | -3.53698600 | 0.76925300 | -0.30946700 |
| H | -2.59842200 | 0.71912900 | -0.66677100 |
| H | -4.16244800 | 0.87026000 | -1.04141400 |
| P | 0.23050700 | -0.19485600 | 0.08148400 |
| O | 0.54872800 | -0.14219600 | 1.63108900 |
| O | 0.81558200 | -1.60592200 | -0.35464900 |
| O | -1.26244400 | -0.05638500 | -0.10276800 |
| C | 1.79566300 | -0.56381500 | 2.26140700 |
| H | 1.66556100 | -0.34960200 | 3.31838500 |
| H | 1.94032400 | -1.63042900 | 2.10093100 |
| H | 2.63110700 | 0.00206200 | 1.85424800 |
| C | 1.04176700 | -2.06663500 | -1.70808100 |
| H | 1.34135300 | -3.10722100 | -1.61533300 |
| H | 0.12208400 | -2.00103000 | -2.29213800 |
| H | 1.84328300 | -1.48896500 | -2.16638800 |
| C | -3.81169300 | -0.49835900 | 0.44838800 |
| H | -2.85452900 | -0.97618800 | 0.74154500 |
| H | -4.34198400 | -1.11701300 | -0.27908600 |
| H | -4.44385700 | -0.11392300 | 1.24164400 |

**Table B17** Cartesian coordinates of int3_2.

| Atomic Type | Coordinate (Angstroms) | | |
|---|---|---|---|
| | X | Y | Z |
| C | 1.72361100 | 0.42096700 | -0.39488900 |
| H | 1.99250800 | 0.23849000 | -1.44621700 |
| C | 1.62867200 | 1.95170400 | -0.19629500 |
| H | 2.67704100 | 2.28001400 | -0.25447300 |
| O | 2.67901400 | -0.19197000 | 0.47153300 |
| H | 3.55021800 | 0.18290700 | 0.29749500 |
| P | 0.17884600 | -0.56851200 | -0.13898900 |
| O | -0.13438000 | -0.72421500 | 1.41817100 |
| O | 0.53236300 | -2.08023000 | -0.54579700 |
| O | -1.00279500 | 0.02100800 | -0.84519400 |
| C | 0.60350900 | -1.55022000 | 2.36449100 |
| H | 0.02040100 | -1.53108900 | 3.28244900 |
| H | 0.68129800 | -2.56701400 | 1.98208500 |
| H | 1.59253900 | -1.12794900 | 2.52648300 |
| C | 0.90463300 | -2.49537900 | -1.87820000 |
| H | 0.82167000 | -3.57985300 | -1.89068100 |
| H | 0.23008600 | -2.06500400 | -2.62097200 |
| H | 1.93726900 | -2.20898700 | -2.08586700 |
| C | 0.87987000 | 2.64416800 | -1.34354800 |
| C | 1.09802200 | 2.36628800 | 1.18134700 |
| H | 0.93407600 | 3.72850500 | -1.22204500 |
| H | 1.31829400 | 2.39903700 | -2.31539400 |
| H | -0.17103100 | 2.35078800 | -1.36760700 |
| H | 1.22951600 | 3.44145900 | 1.32401700 |
| H | 0.03150400 | 2.14637400 | 1.28324100 |
| H | 1.62823200 | 1.85468800 | 1.98693900 |
| C | -3.32041600 | 0.25537700 | -0.16614500 |
| O | -4.86299100 | 0.48297700 | 0.23065500 |
| H | -5.36528900 | 1.01137700 | -0.41266100 |
| H | -5.35043200 | -0.33521800 | 0.42597400 |
| H | -2.96647300 | 1.26939100 | -0.28162700 |
| H | -2.93479800 | -0.24557400 | 0.71114000 |
| H | -3.33641700 | -0.33264000 | -1.07296300 |

**Table B18** Cartesian coordinates of ahp.

| Atomic Type | Coordinate (Angstroms) | | |
|---|---|---|---|
| | X | Y | Z |
| C | 1.15535900 | -0.78866200 | 0.47866000 |
| H | 0.83951000 | -1.78467500 | 0.82051700 |
| C | 2.40370300 | -0.92607000 | -0.39064600 |
| H | 2.20601800 | -1.57775400 | -1.24370900 |
| H | 2.72785900 | 0.04859200 | -0.76160300 |
| H | 3.21942400 | -1.36547500 | 0.19384600 |
| O | 1.35504900 | 0.07599200 | 1.60088600 |
| H | 2.14395500 | -0.21188100 | 2.07293700 |
| P | -0.27144600 | -0.13121400 | -0.49505800 |
| O | 0.06268600 | 1.39965000 | -0.81997900 |
| O | -1.50491400 | 0.01590300 | 0.54271400 |
| O | -0.53149900 | -0.96962500 | -1.68633300 |
| C | -0.11477800 | 2.51564100 | 0.08051700 |
| H | 0.14030300 | 3.40258000 | -0.49698800 |
| H | -1.15238200 | 2.56801500 | 0.41070100 |
| H | 0.54811300 | 2.41490900 | 0.93952400 |
| C | -2.40222600 | -1.08033900 | 0.79571600 |
| H | -3.29814800 | -0.64865100 | 1.23907600 |
| H | -2.65360000 | -1.59280200 | -0.13421300 |
| H | -1.95229300 | -1.78341800 | 1.50199000 |

**Table B19**  Cartesian coordinates of ahp_2.

| Atomic Type | Coordinate (Angstroms) | | |
|---|---|---|---|
| | X | Y | Z |
| C | 0.71427200 | -0.16700600 | 0.89709500 |
| H | 0.56608700 | -1.10385600 | 1.45456900 |
| C | 2.17828400 | -0.13554300 | 0.40188300 |
| H | 2.76238600 | 0.02865900 | 1.32138500 |
| O | 0.40053100 | 0.95121200 | 1.73554700 |
| H | 0.96621800 | 0.91786000 | 2.51458100 |
| P | -0.59721400 | -0.19671600 | -0.41477300 |
| O | -0.81792400 | 1.31075200 | -0.89880300 |
| O | -1.97680000 | -0.49601200 | 0.38421300 |
| O | -0.28911100 | -1.14507100 | -1.50950700 |
| C | -1.60631900 | 2.32457300 | -0.23865500 |
| H | -1.71048300 | 3.13347400 | -0.95999100 |
| H | -2.58686100 | 1.92744400 | 0.02426000 |
| H | -1.08941200 | 2.67194000 | 0.65503000 |
| C | -2.47777500 | -1.83719900 | 0.53000400 |
| H | -3.53966200 | -1.74721300 | 0.75419700 |
| H | -2.33458500 | -2.40354400 | -0.39131500 |
| H | -1.97459100 | -2.34211300 | 1.35949400 |
| C | 2.62245500 | -1.48353900 | -0.18377900 |
| C | 2.47868400 | 1.03166900 | -0.54743100 |
| H | 3.68923900 | -1.45334500 | -0.42164000 |
| H | 2.46450700 | -2.30000500 | 0.52846700 |
| H | 2.06901500 | -1.71838900 | -1.09431200 |
| H | 3.55614000 | 1.10777900 | -0.71779100 |
| H | 1.99707800 | 0.88620800 | -1.51768600 |
| H | 2.13195000 | 1.98106500 | -0.13394700 |

**APPENDIX C**



(H₂O)

(H₃O⁺)

(MeOH₂⁺)

(MeOH)

(tmp)
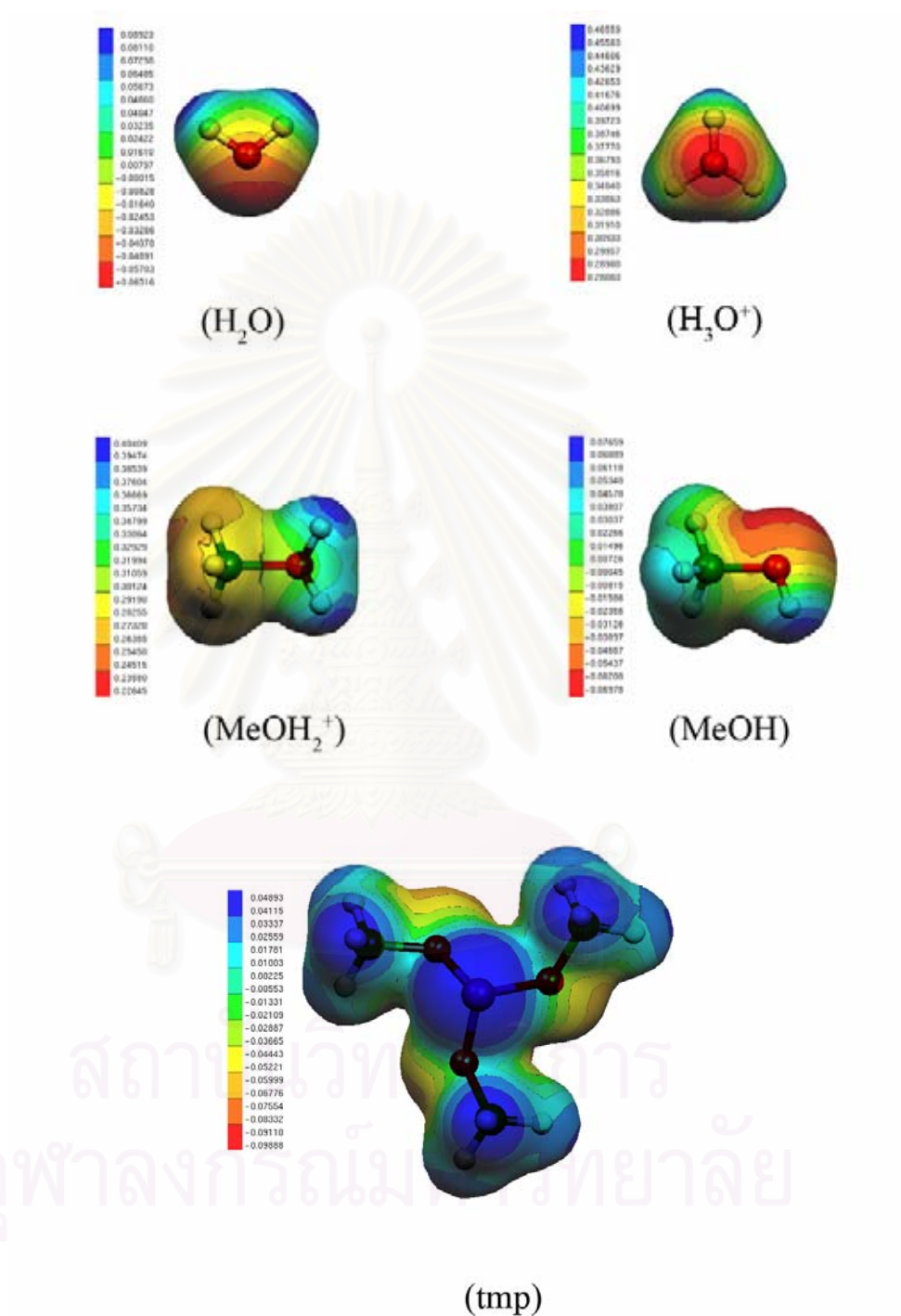
**Figure C1** Molecular electrostatic potential energy of water (H$_2$O), hydronium ion (H$_3$O$^+$), protonated-methanal (MeOH$_2^+$), methanal (MeOH) and trimetylphosphite (tmp).
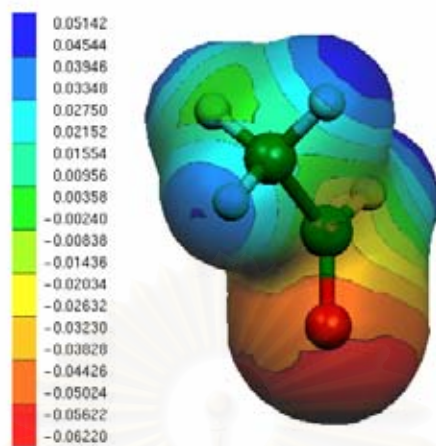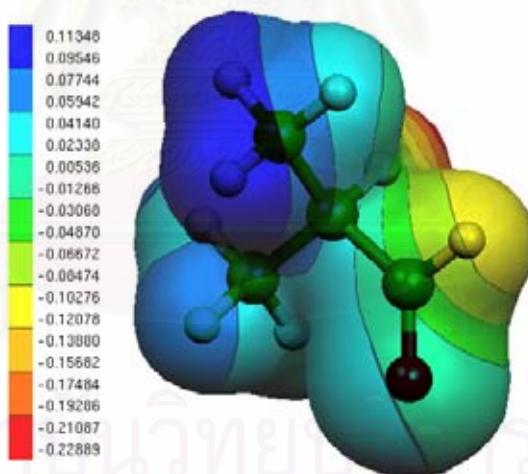
**Figure C2** Molecular electrostatic potential energy of acetaldehyde (ald), *i*-propyl aldehyde (ald_2).
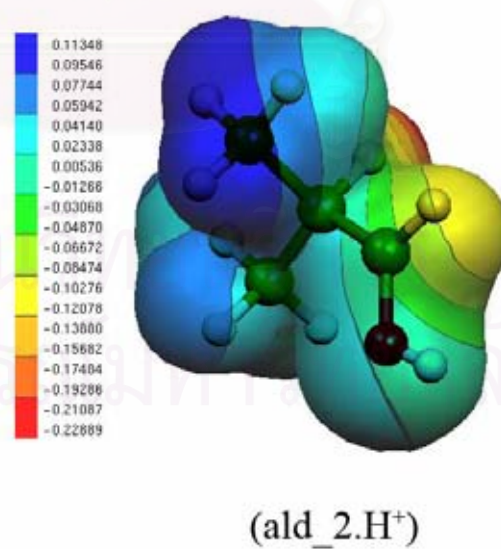
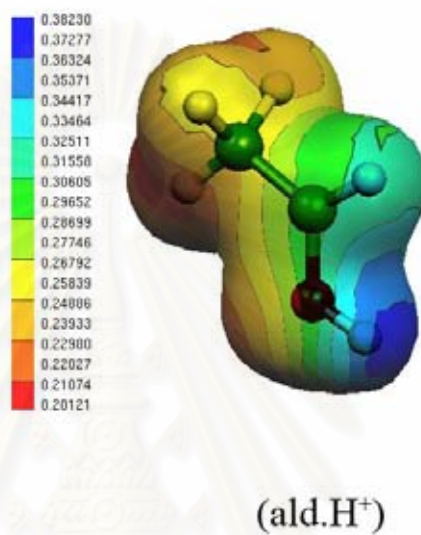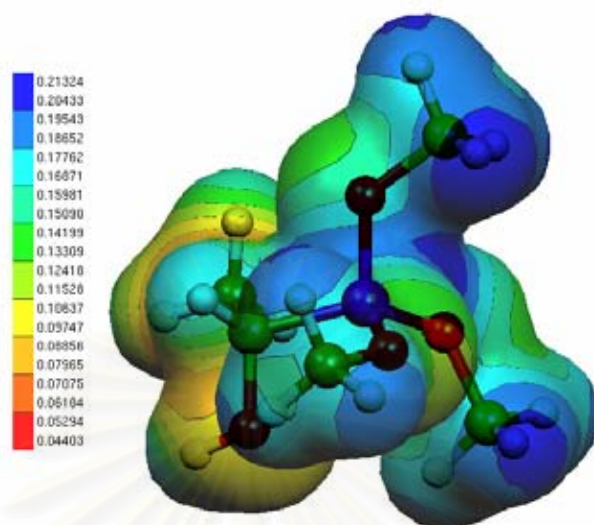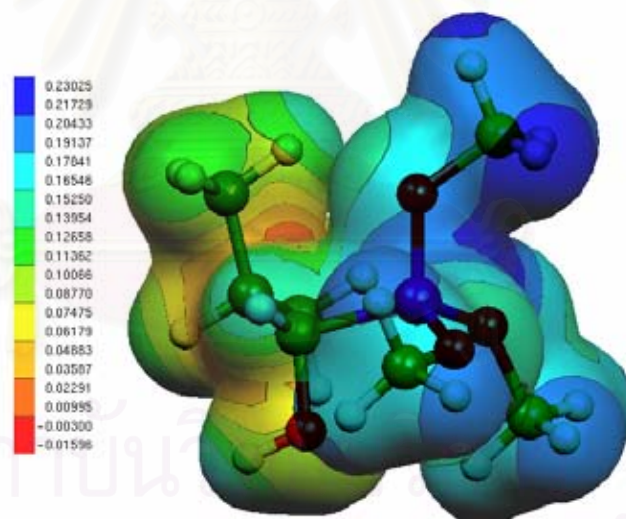**Figure C3**   Molecular electrostatic potential energy of protonated acetaldehyde (ald.H⁺), protonated *i*-propyl aldehyde (ald_2.H⁺).

(int1)



(int1_2)

**Figure C4** Molecular electrostatic potential energy of intermediates int1, int1_2 in acetaldehyde (top) and *i*-propyl aldehyde (bottom).
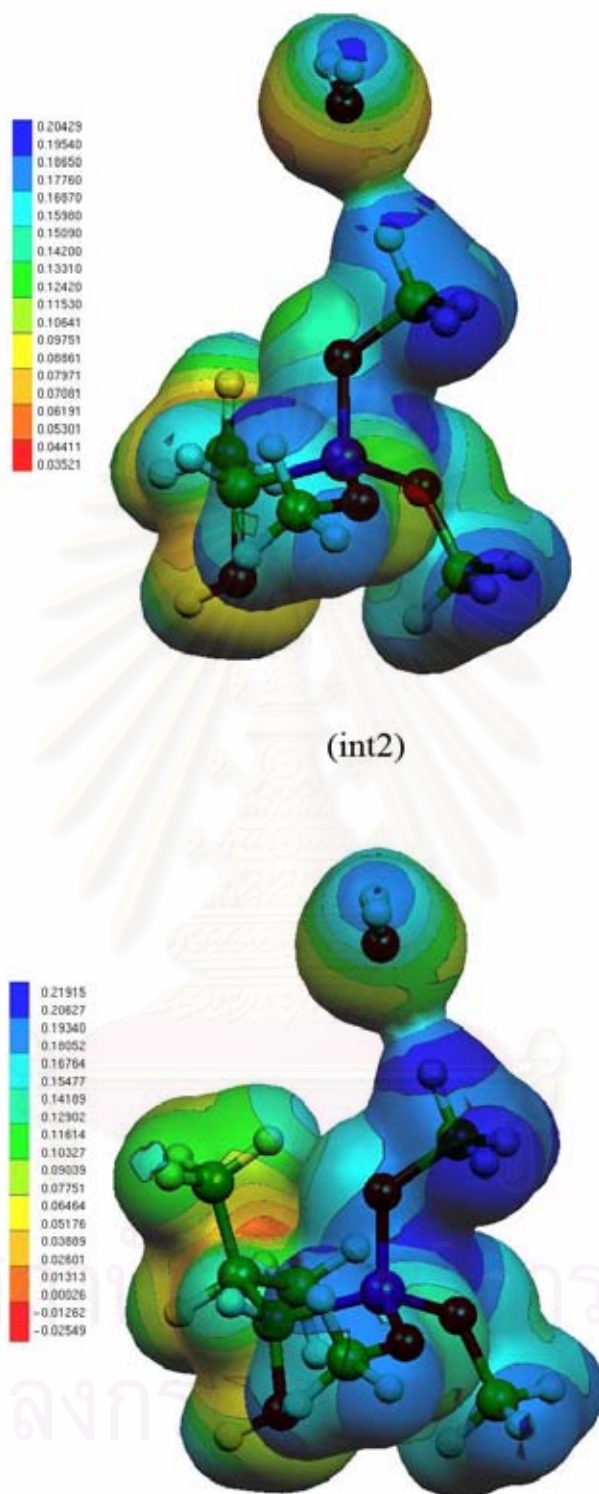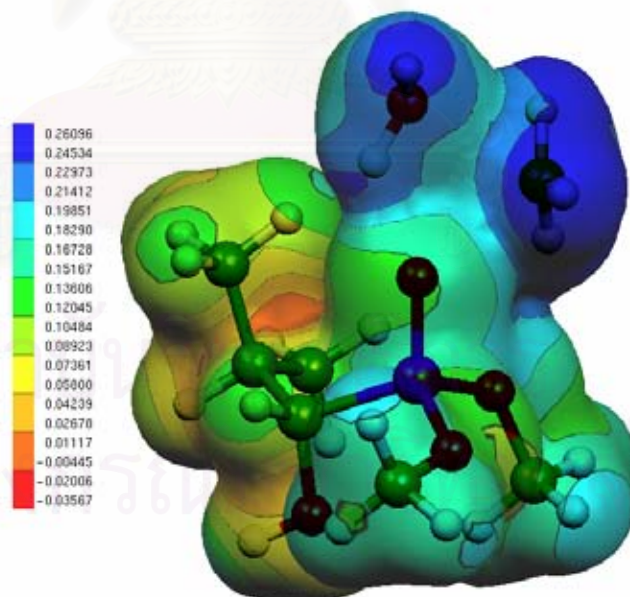
**Figure C5** Molecular electrostatic potential energy of intermediates int2, int2_2 in acetaldehyde (top) and *i*-propyl aldehyde (bottom).
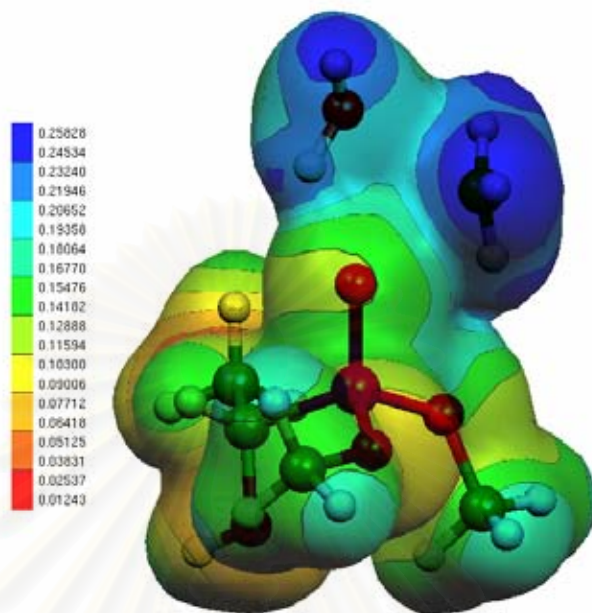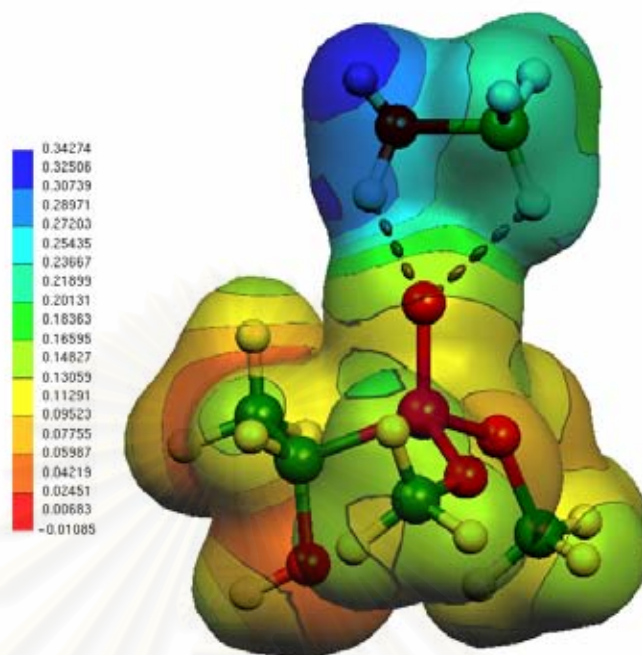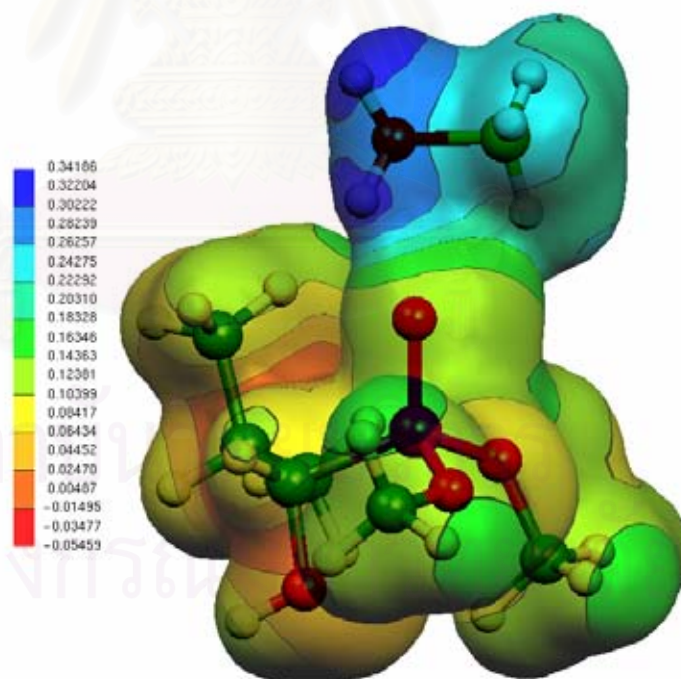
**Figure C6** Molecular electrostatic potential energy of transition states TS, TS_2 in acetaldehyde (top) and *i*-propyl aldehyde (bottom).

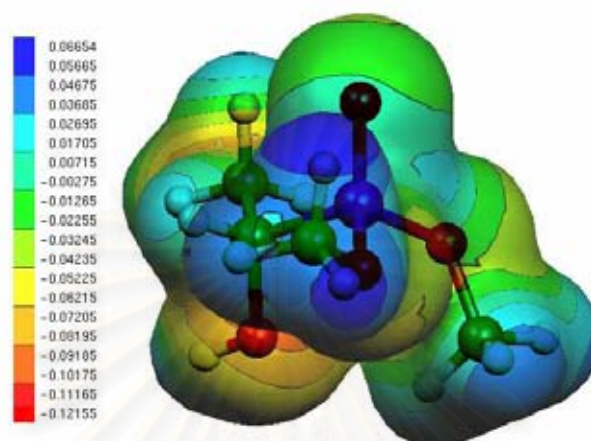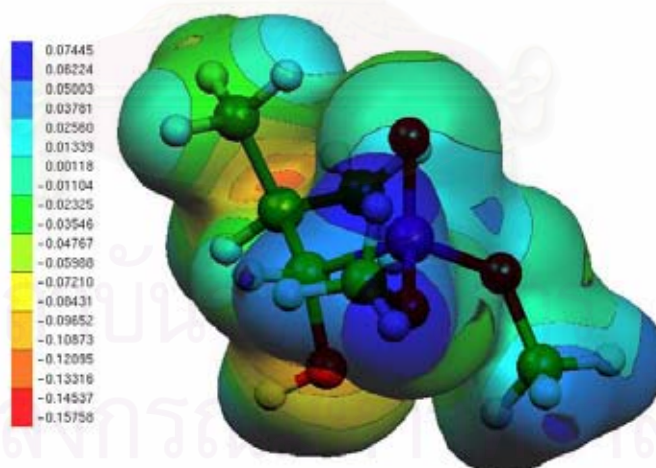**Figure C7** Molecular electrostatic potential energy of intermediates int3, int3_2 in acetaldehyde (top) and *i*-propyl aldehyde (bottom).

(ahp)



(ahp_2)

**Figure C8** Molecular electrostatic potential energy of α-hydroxy phosphonates ahp, ahp_2 in acetaldehyde (top) and *i*-propyl aldehyde (bottom).

## VITA

**NAME, NICKNAME**:    Miss Kanchana  Dulya, Kae

**BIRTH DATE**:    May $2^{nd}$, 1980

**BIRTH PLACE**:    Ayutthaya Province, Thailand

**EDUCATION**:

| YEAR | INSTITUTION | DEGREE/DIPLOMA |
|---|---|---|
| 1999 | Saraburiwitthayakom | High School |
| 2003 | Kasetsart Univ. | B.S. (Physics) |
| 2006 | Chulalongkorn Univ. | M.S. |
| | (Petrochemistry and Polymer Science) | |

**WORK EXPERIENCE**:  2003    Reliability and Quality Control Engineer

                      NEC TOKIN Electronics (Thailand) Co., Ltd.

               2005    Quality Control Supervisor

                      NIPRO Thailand Co., Ltd.

**ADDRESS**:    327/6, Moo 9, Champa, Tharua, Ayutthaya, 13130

               Thailand. Tel. 08-1483-5591.

**E-MAIL:**    kandulya@yahoo.com